From vortices to turbulence: dynamics in strongly interacting Fermi superfluids

Gabriel Wlazłowski

Warsaw University of Technology
University of Washington

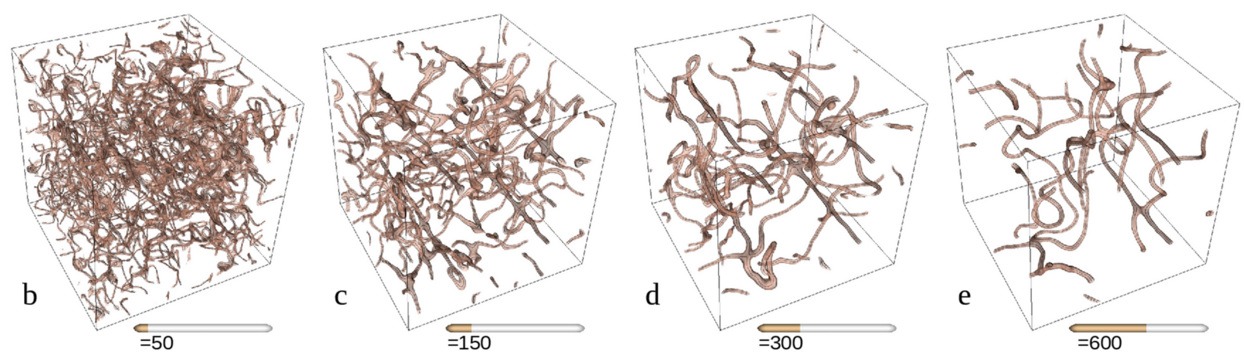

NATIONAL SCIENCE CENTRE
POLAND

LUMI

Compressible Turbulence: From Cold Atoms to Neutron Star Mergers
INT-25-2a, June 23 – 27, 2025, Seattle

Quantum turbulence

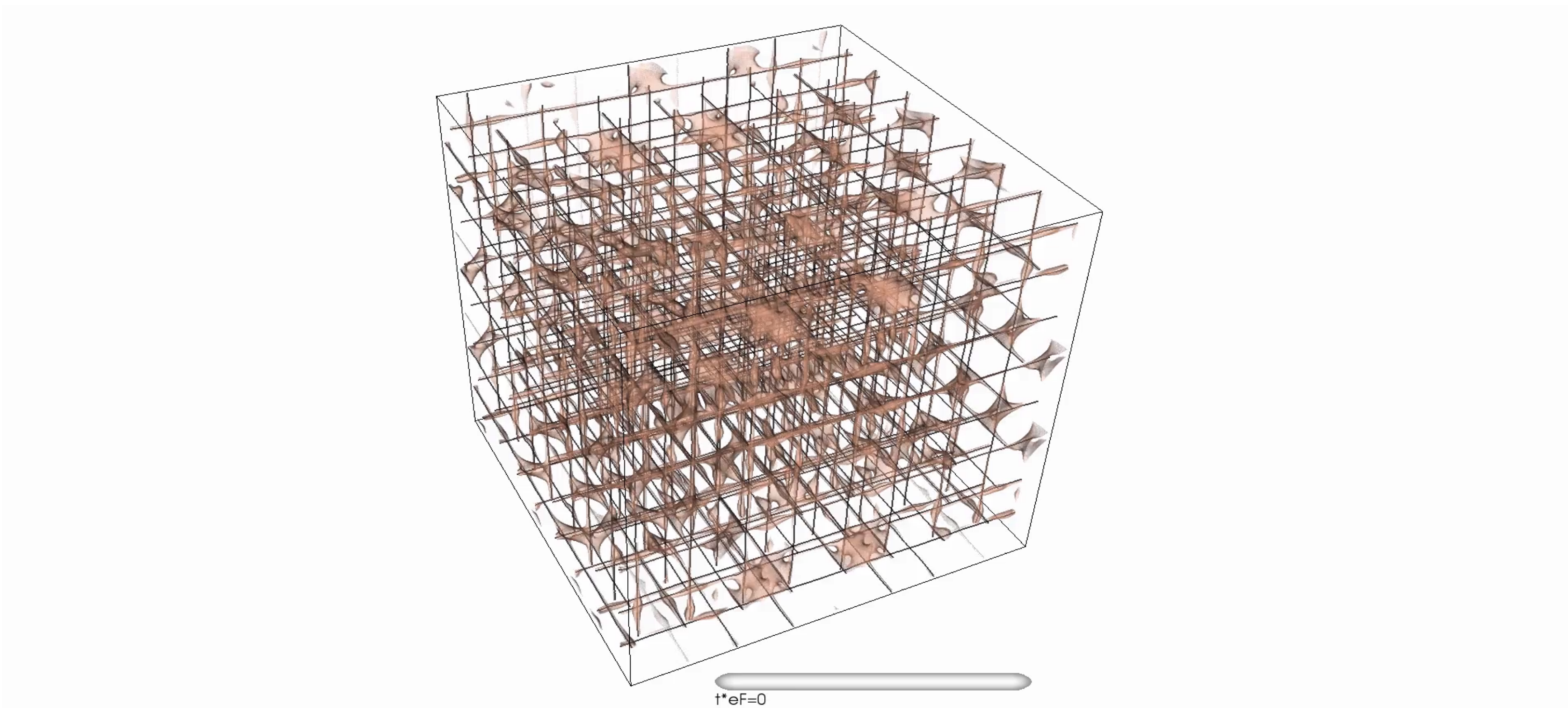

System: *unitary Fermi gas (spin-symmetric)*
number of atoms = 26,790
Method: *Time-Dependent Density Functional Theory*
PNAS Nexus, pgae160 (2024)

Computation
on spatial grid

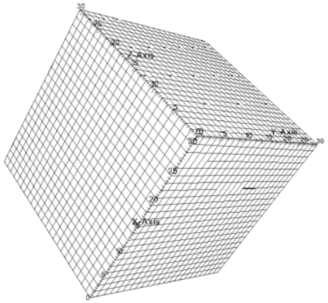

(the largest system in 3D we considered had 108,532 atoms)

Quantum turbulence in Bose systems

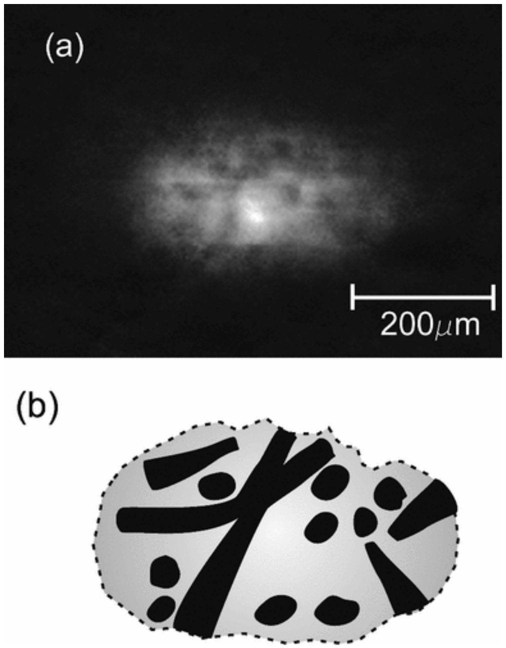

E. A. L. Henn, J. A. Seman, G. Roati, K. M. F. Magalhães, and V. S. Bagnato, Phys. Rev. Lett. 103, 045301 (2009)

…

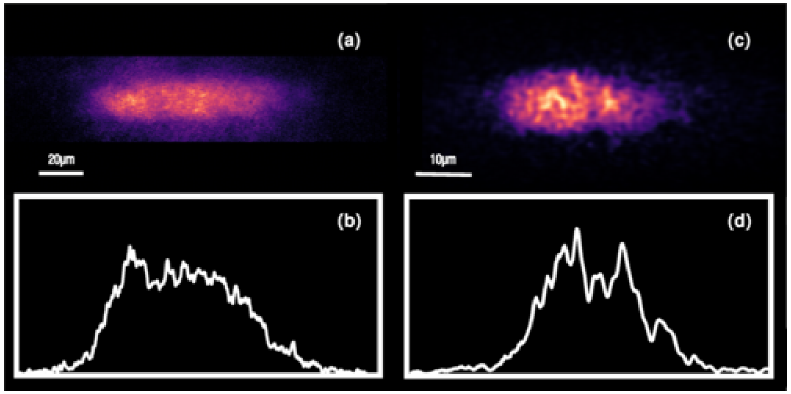

H. A. J. Middleton-Spencer, A. D. G. Orozco, L. Galantucci, M. Moreno, N. G. Parker, L. A. Machado, V. S. Bagnato, and C. F. Barenghi, Phys. Rev. Research 5, 043081 (2023)

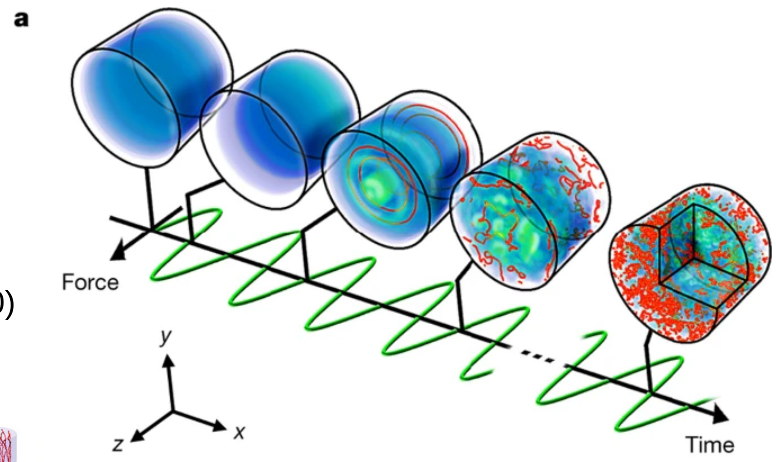

Nir Navon, Alexander L. Gaunt, Robert P. Smith & Zoran Hadzibabic Nature 539, p. 72–75 (2016)

Reviews:

- L. Madeira, et al., Ann. Rev. of Cond. Mat. Phys., 11 (2020)
- M.C. Tsatsos, et al., Phys. Rep. 622, 1 (2016).
- M. Tsubota, et al., J. Low. Temp. Phys. 188, 119 (2017)

…

… *superfluid helium* …

… J. T. Mäkinen, et.al., Nat. Phys. 19, 898 (2023)

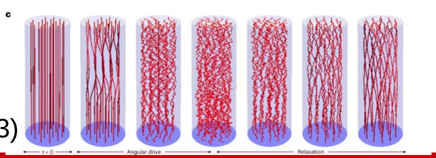

Superfluidity across BEC-BCS crossover

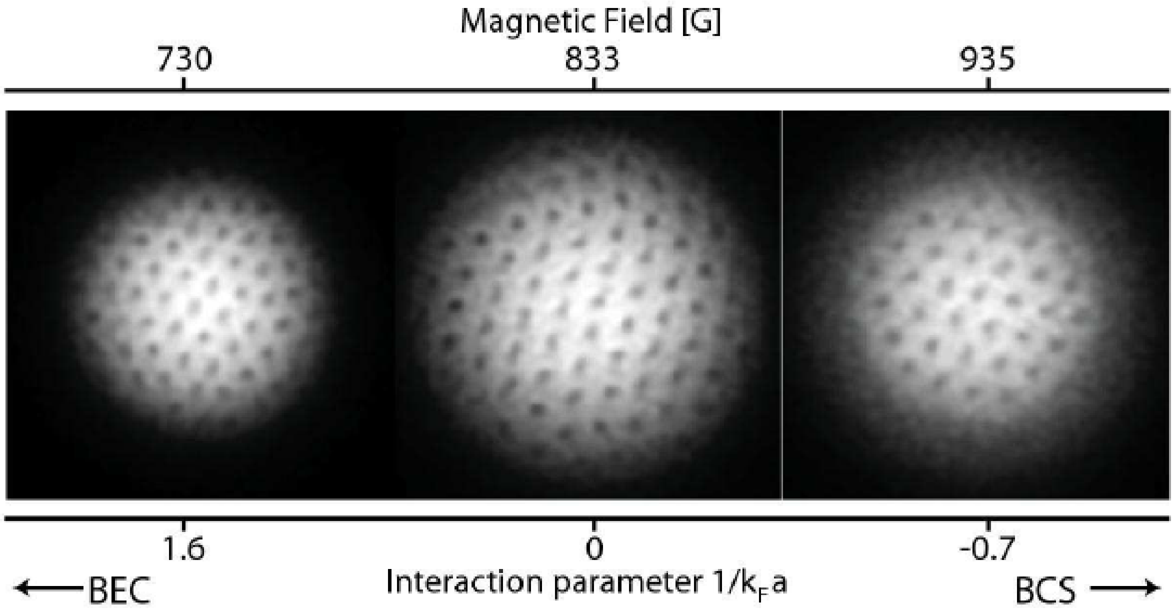

FIG. 36 Vortex lattice in a rotating gas of ^{6}Li precisely at the Feshbach resonance and on the BEC and BCS side. Reprinted with permission from Zwierlein *et al.* (2005).

M. W. Zwierlein, J. R. Abo-Shaeer, A. Schirotzek, C. H. Schunck, and W. Ketterle, Nature 435, 1047 (2005).

Scientific question:
What is **impact of quantum statistics** on superfluid (turbulent) dynamics?

Comparing Bose & Fermi superfluids

L=0, S=0
(s-wave superfluidity)

→ the simplest form of superfluidity in Fermi systems

→ BEC-BCS crossover allows to make **direct comparisons within the same system!**

^{4}He

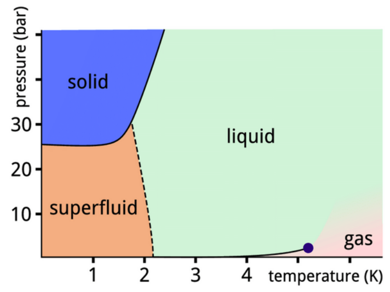

^{3}He

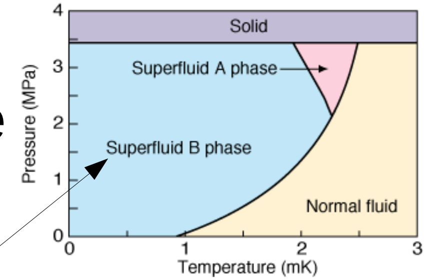

L=1, S=1
(p-wave, spin-triplet)

→ additional level of complication

Synergy: theory & experiment

Experiments:

$$\frac{T}{T_F} \gtrsim 0.05$$

$$|ak_F| \gtrsim 1$$

~exp. limitation

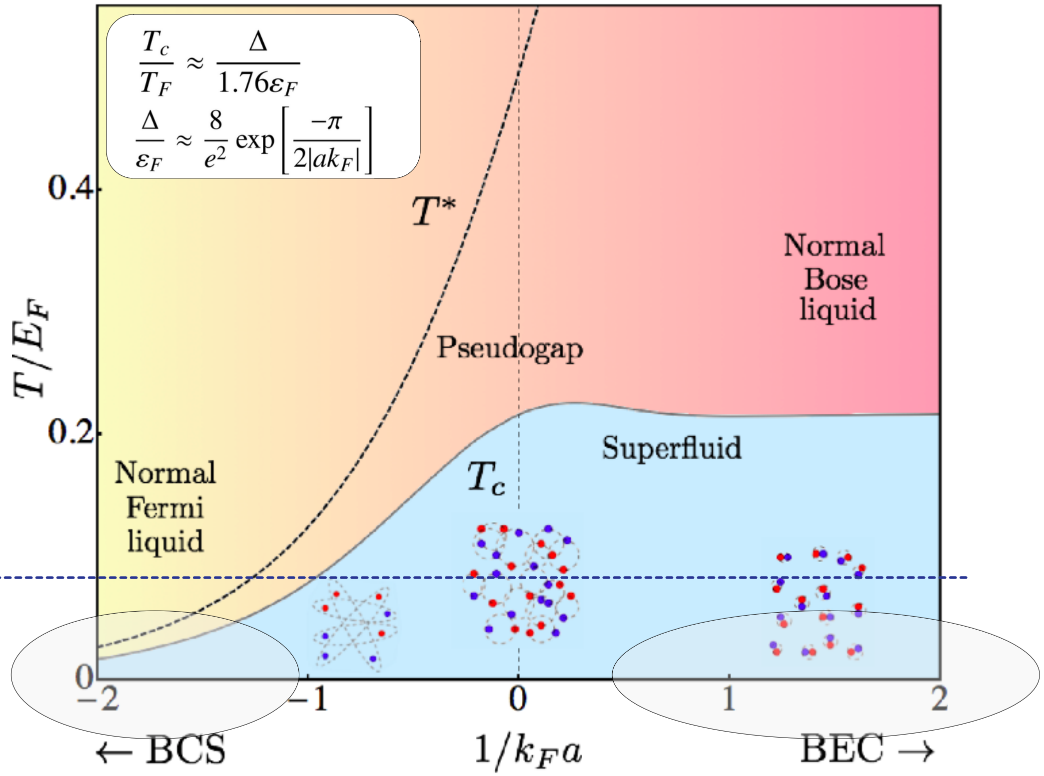

Mean-field Theory

Regime of validity of BdG theory

Regime of validity of GPE

(note: BdG for uniform system= BCS theory)

PHYSICS.WUT

Synergy: theory & experiment

Experiments:

$$\frac{T}{T_F} \gtrsim 0.05$$

$$\downarrow$$

$$|ak_F| \gtrsim 1$$

~exp. limitation

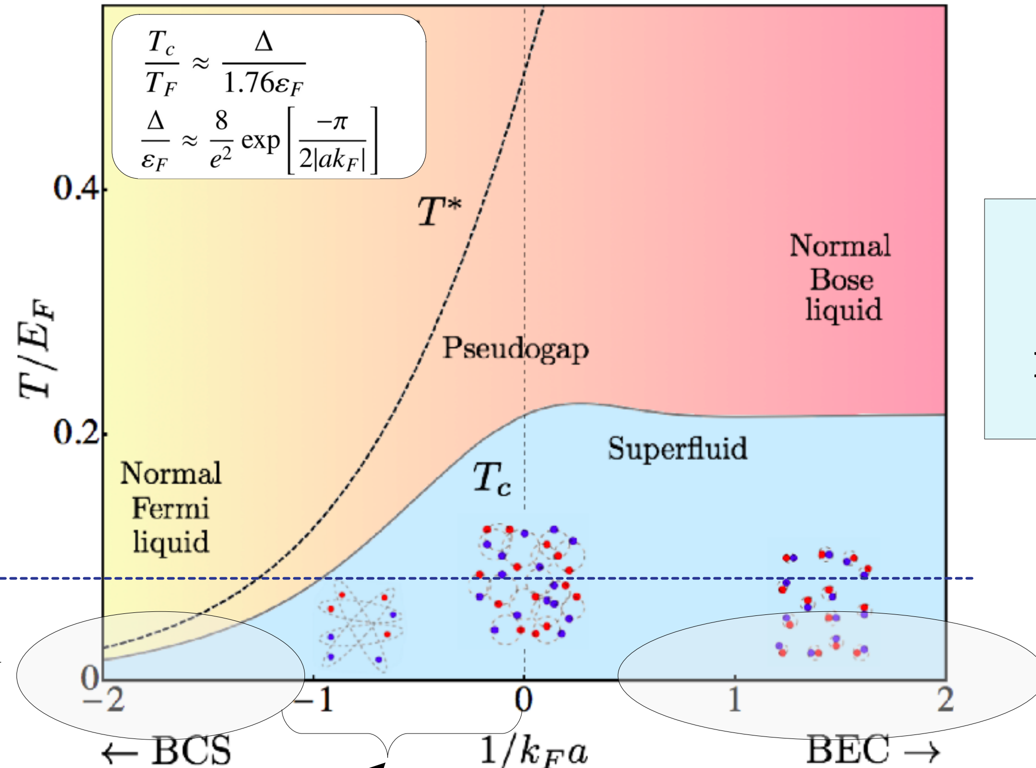

Regime of validity of BdG theory

(note: BdG for uniform system= BCS theory)

Mean-field Theory

Density Functional Theory

Regime of validity of GPE

DFT is, in principle, exact theory (due to Hohenberg-Kohn theorem)…
… in practice not – we need to construct the energy functional (no mathematical recipe how to derive it)

Nature 514, 550 (2014)

… *Twelve papers on the top-100 list relate to it* [DFT], *including 2 of the top 10.*

Many extensions: time-dependent formalism, finite temperature, normal/superconducting systems, non-relativistic/relativistic, …

General purpose framework

SLDA-type functional

Superfluid **L**ocal **D**ensity **A**pproximation

$$\boxed{E_0 = \int \mathcal{E}[n_\sigma(\boldsymbol{r}), \tau_\sigma(\boldsymbol{r}), \boldsymbol{j}_\sigma, \nu(\boldsymbol{r})]\, d\boldsymbol{r}}$$

The Fermi-Dirac distribution function

normal density

$$n_\sigma(\boldsymbol{r}) = \sum_{|E_n|<E_c} |v_{n,\sigma}(\boldsymbol{r})|^2 f_\beta(-E_n),$$

kinetic density

$$\tau_\sigma(\boldsymbol{r}) = \sum_{|E_n|<E_c} |\nabla v_{n,\sigma}(\boldsymbol{r})|^2 f_\beta(-E_n),$$

current density

$$\boldsymbol{j}_\sigma(\boldsymbol{r}) = \sum_{|E_n|<E_c} \mathrm{Im}[v_{n,\sigma}(\boldsymbol{r})\nabla v^*_{n,\sigma}(\boldsymbol{r})] f_\beta(-E_n),$$

anomalous density

$$\nu(\boldsymbol{r}) = \frac{1}{2}\sum_{|E_n|<E_c} \left[u_{n,a}(\boldsymbol{r})v^*_{n,b}(\boldsymbol{r}) - u_{n,b}(\boldsymbol{r})v^*_{n,a}(\boldsymbol{r})\right] f_\beta(-E_n).$$

Energy cut-off scale (need for regularization)

Denisties are **parametrized** via Bogoliubov quasiparticle wave functions

quasiparticle = mixture of hole particle

$$\varphi_\eta(\boldsymbol{r},t) = [u_\eta(\boldsymbol{r},t), v_\eta(\boldsymbol{r},t)]^T$$

$$\int \varphi^\dagger_\eta(\boldsymbol{r},t)\varphi_{\eta'}(\boldsymbol{r},t)\, d^3\boldsymbol{r} = \delta_{\eta,\eta'}$$

+ orthonormality condition (Pauli principle)

Additional density required by DFT theorem for systems with broken U(1) symmetry

SLDA (and BdG) allows for solutions: **n≠0 and ν=0**

→ ***Cooper pair breaking*** → ***effectively normal component***

SLDA-type functional

$$E_0 = \int \mathcal{E}[n_\sigma(\boldsymbol{r}), \tau_\sigma(\boldsymbol{r}), \boldsymbol{j}_\sigma, \nu(\boldsymbol{r})]\, d\boldsymbol{r}$$

$$\Big\downarrow \text{minimization}$$

By construction minimization of the SLDA-type functional leads to equations that are mathematically equivalent to BdG or HFB equations

$$\begin{pmatrix} h_\uparrow(\boldsymbol{r}) - \mu_\uparrow & \Delta(\boldsymbol{r}) \\ \Delta^*(\boldsymbol{r}) & -h_\downarrow^*(\boldsymbol{r}) + \mu_\downarrow \end{pmatrix} \begin{pmatrix} u_{n,\uparrow}(\boldsymbol{r}) \\ v_{n,\downarrow}(\boldsymbol{r}) \end{pmatrix} = E_n \begin{pmatrix} u_{n,\uparrow}(\boldsymbol{r}) \\ v_{n,\downarrow}(\boldsymbol{r}) \end{pmatrix}$$

$$h_\sigma = -\boldsymbol{\nabla} \frac{\delta E_0}{\delta \tau_\sigma} \boldsymbol{\nabla} + \frac{\delta E_0}{\delta n_\sigma} - \frac{i}{2} \left\{ \frac{\delta E_0}{\delta \boldsymbol{j}_\sigma}, \boldsymbol{\nabla} \right\}, \quad \Delta = -\frac{\delta E_0}{\delta \nu^*}.$$

SLDA-type functional

$$E_0 = \int \mathcal{E}[n_\sigma(\boldsymbol{r}), \tau_\sigma(\boldsymbol{r}), \boldsymbol{j}_\sigma, \nu(\boldsymbol{r})]\, d\boldsymbol{r}$$

minimization

By construction minimization of the SLDA-type functional leads to equations that are mathematically equivalent to BdG or HFB equations

$$\begin{pmatrix} h_\uparrow(\boldsymbol{r}) - \mu_\uparrow & \Delta(\boldsymbol{r}) \\ \Delta^*(\boldsymbol{r}) & -h_\downarrow^*(\boldsymbol{r}) + \mu_\downarrow \end{pmatrix} \begin{pmatrix} u_{n,\uparrow}(\boldsymbol{r}) \\ v_{n,\downarrow}(\boldsymbol{r}) \end{pmatrix} = E_n \begin{pmatrix} u_{n,\uparrow}(\boldsymbol{r}) \\ v_{n,\downarrow}(\boldsymbol{r}) \end{pmatrix}$$

$$h_\sigma = -\boldsymbol{\nabla}\frac{\delta E_0}{\delta \tau_\sigma}\boldsymbol{\nabla} + \frac{\delta E_0}{\delta n_\sigma} - \frac{i}{2}\left\{\frac{\delta E_0}{\delta \boldsymbol{j}_\sigma}, \boldsymbol{\nabla}\right\}, \quad \Delta = -\frac{\delta E_0}{\delta \nu^*}.$$

From point of view of DFT this step represents approximation, called *adiabatic approximation*

$$\begin{pmatrix} h_\uparrow(\boldsymbol{r},t) - \mu_\uparrow & \Delta(\boldsymbol{r},t) \\ \Delta^*(\boldsymbol{r},t) & -h_\downarrow^*(\boldsymbol{r},t) + \mu_\downarrow \end{pmatrix} \begin{pmatrix} u_{n,\uparrow}(\boldsymbol{r},t) \\ v_{n,\downarrow}(\boldsymbol{r},t) \end{pmatrix} = i\hbar\frac{\partial}{\partial t} \begin{pmatrix} u_{n,\uparrow}(\boldsymbol{r},t) \\ v_{n,\downarrow}(\boldsymbol{r},t) \end{pmatrix}$$

DFT method from practical point of view:

DFT method allows for the description of many-body quantum systems with higher accuracy than the mean-field method while keeping the computational complexity at the same level as for the mean-field method.

SLDA-type functional

for ultra-cold atoms

$$E_0 = \int \mathcal{E}[n(\boldsymbol{r}), \tau(\boldsymbol{r}), \boldsymbol{j}(\boldsymbol{r}), \nu(\boldsymbol{r})] d\boldsymbol{r}$$

Dimensionless functional parameters

$$\{A_\lambda, B_\lambda, C_\lambda\}$$

$$\lambda = a k_F$$

Densities $n(\boldsymbol{r})$, $\tau(\boldsymbol{r})$, $\nu(\boldsymbol{r})$ are defined via $[u_\eta(\boldsymbol{r},t), v_\eta(\boldsymbol{r},t)]^T$

$$\mathcal{E} = \frac{A_\lambda}{2}\left(\tau - \frac{\boldsymbol{j}^2}{n}\right) + \frac{3}{5} B_\lambda n \varepsilon_F + \frac{C_\lambda}{n^{1/3}} |\nu|^2 + \frac{\boldsymbol{j}^2}{2n}$$

dimensional analysis + symmetries

Kinetic term (intrinsic)

Potential term

Pairing term

Collective flow energy

Units: $\hbar = m = 1$

SLDA-type functional

for ultra-cold atoms

$$E_0 = \int \mathcal{E}[n(\boldsymbol{r}), \tau(\boldsymbol{r}), \boldsymbol{j}(\boldsymbol{r}), \nu(\boldsymbol{r})] d\boldsymbol{r}$$

Dimensionless functional parameters

$$\{A_\lambda, B_\lambda, C_\lambda\}$$

$$\lambda = ak_F$$

Densities $n(\boldsymbol{r}),\ \tau(\boldsymbol{r}),\ \nu(\boldsymbol{r})$ are defined via $[u_\eta(\boldsymbol{r},t), v_\eta(\boldsymbol{r},t)]^T$

$$\mathcal{E} = \underbrace{\frac{A_\lambda}{2}\left(\tau - \frac{\boldsymbol{j}^2}{n}\right)}_{\text{Kinetic term (intrinsic)}} + \underbrace{\frac{3}{5} B_\lambda n \varepsilon_F}_{\text{Potential term}} + \underbrace{\frac{C_\lambda}{n^{1/3}} |\nu|^2}_{\text{Pairing term}} + \underbrace{\frac{\boldsymbol{j}^2}{2n}}_{\text{Collective flow energy}}$$

dimensional analysis + symmetries

Units: $\hbar = m = 1$

Example: The simplest choice

BdG (mean-field)
$A_\lambda \to 1$
$B_\lambda \to 0$
$C_\lambda \to \dfrac{4\pi\hbar^2}{(3\pi^2)^{1/3} m} \overbrace{ak_F}^{\lambda}$

$$\mathcal{E}_{\mathrm{BdG}} = \frac{\tau}{2} + 4\pi a |\nu(\boldsymbol{r})|^2$$

$\downarrow$ *minimization*

$$\begin{pmatrix} -\frac{\hbar^2}{2}\nabla^2 - \mu & \Delta(\boldsymbol{r}) \\ \Delta^*(\boldsymbol{r}) & \frac{\hbar^2}{2}\nabla^2 + \mu \end{pmatrix} \begin{pmatrix} u_n(\boldsymbol{r}) \\ v_n(\boldsymbol{r}) \end{pmatrix} = E_n \begin{pmatrix} u_n(\boldsymbol{r}) \\ v_n(\boldsymbol{r}) \end{pmatrix}$$

$$\Delta = -4\pi a \sum_{|E_n| < E_c} u_n(\mathbf{r}) v_n^*(\mathbf{r}) \frac{f_\beta(-E_n) - f_\beta(E_n)}{2}$$

There always exists a functional that after minimization provides equations identical to the mean-field equations (zeroth order).

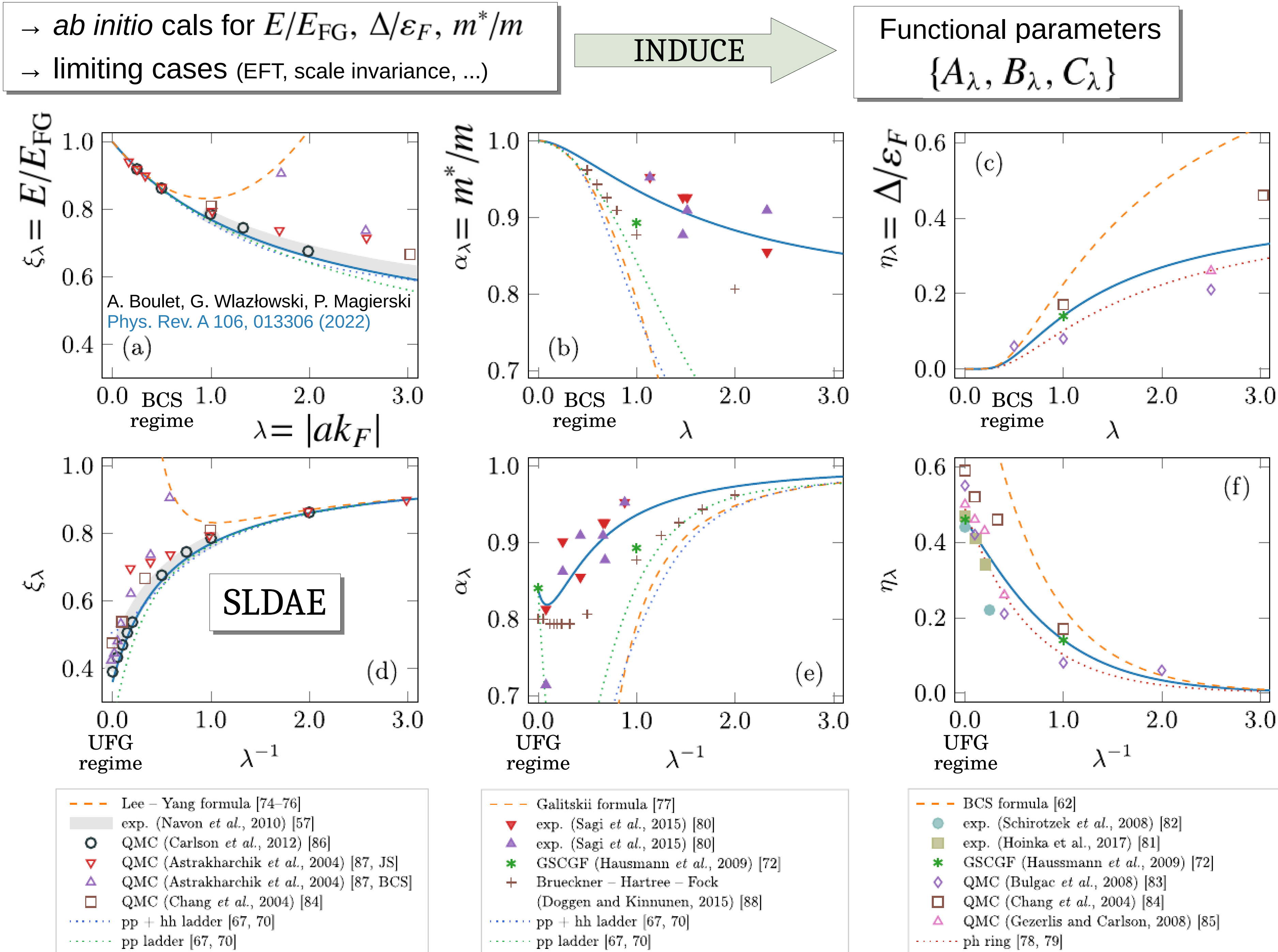
→ ab initio cals for E/E_{FG}, Δ/ε_F, m^*/m
→ limiting cases (EFT, scale invariance, ...)
INDUCE
Functional parameters
$\{A_\lambda, B_\lambda, C_\lambda\}$
$\xi_\lambda = E/E_{FG}$
$\alpha_\lambda = m^*/m$
$\eta_\lambda = \Delta/\varepsilon_F$
A. Boulet, G. Wlazłowski, P. Magierski
Phys. Rev. A 106, 013306 (2022)
(a)
(b)
(c)
(d)
(e)
(f)
BCS regime
$\lambda = |ak_F|$
λ
UFG regime
λ^{-1}
ξ_λ
α_λ
η_λ
SLDAE
Lee – Yang formula [74–76]
exp. (Navon et al., 2010) [57]
QMC (Carlson et al., 2012) [86]
QMC (Astrakharchik et al., 2004) [87, JS]
QMC (Astrakharchik et al., 2004) [87, BCS]
QMC (Chang et al., 2004) [84]
pp + hh ladder [67, 70]
pp ladder [67, 70]
Galitskii formula [77]
exp. (Sagi et al., 2015) [80]
exp. (Sagi et al., 2015) [80]
GSCGF (Hausmann et al., 2009) [72]
Brueckner – Hartree – Fock
(Doggen and Kinnunen, 2015) [88]
pp + hh ladder [67, 70]
pp ladder [67, 70]
BCS formula [62]
exp. (Schirotzek et al., 2008) [82]
exp. (Hoinka et al., 2017) [81]
GSCGF (Haussmann et al., 2009) [72]
QMC (Bulgac et al., 2008) [83]
QMC (Chang et al., 2004) [84]
QMC (Gezerlis and Carlson, 2008) [85]
ph ring [78, 79]

Quantum turbulence in 3D

G. Wlazłowski, M.M.Forbes, S. Sarkar, A. Marek, M. Szpindler, PNAS Nexus, pgae160 (2024)

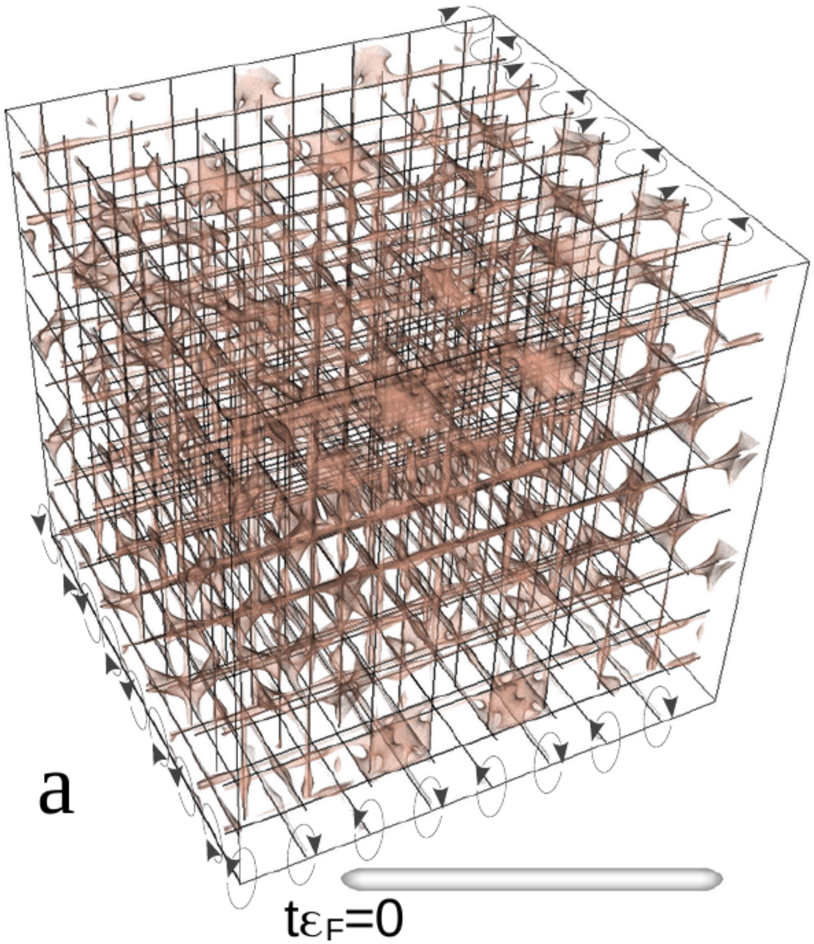

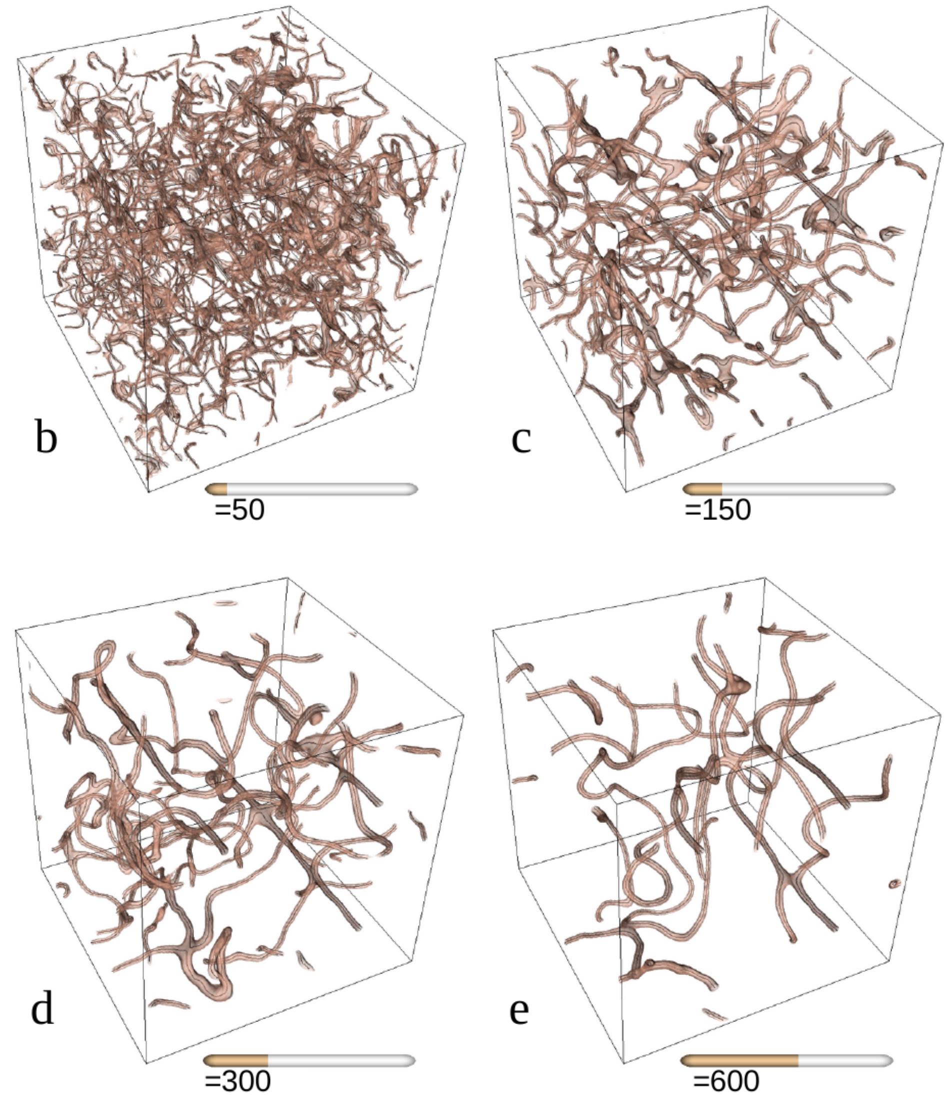

initial state:

→ zero temperature (T = 0)
→ regular lattice of imprinted vortices
in all three directions
→ the lattice consists of alternately arranged
vortices and anti-vortices
→ small long-wavelength perturbations of vortex lines

Quantum turbulence in 3D

G. Wlazłowski, M.M.Forbes, S. Sarkar, A. Marek, M. Szpindler,
PNAS Nexus, pgae160 (2024)

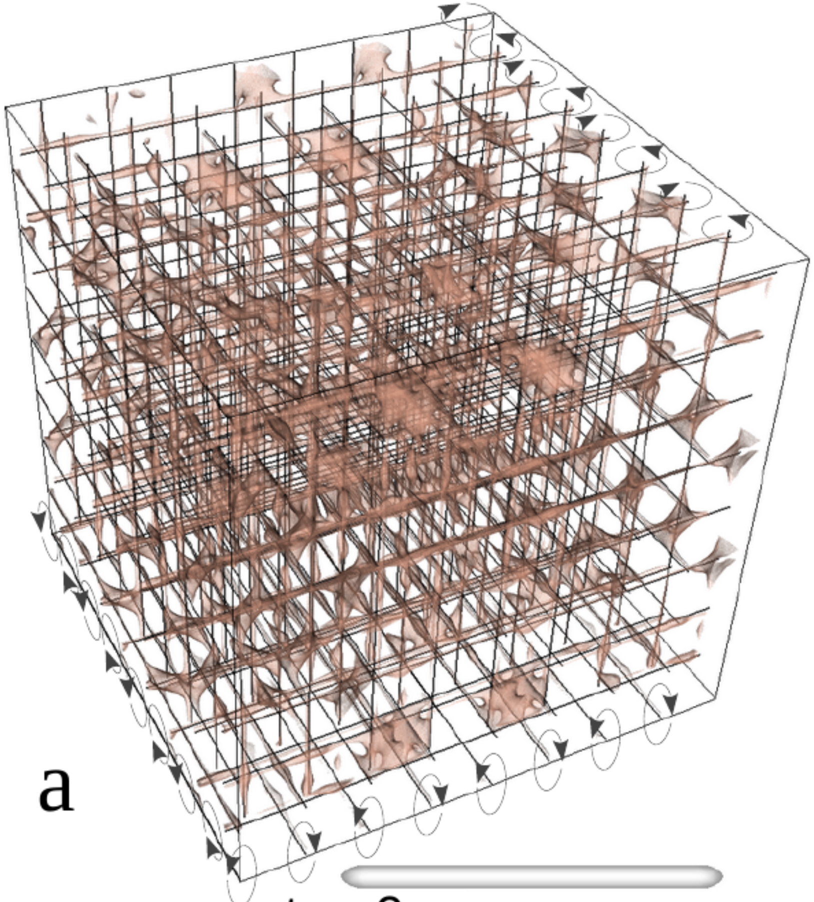

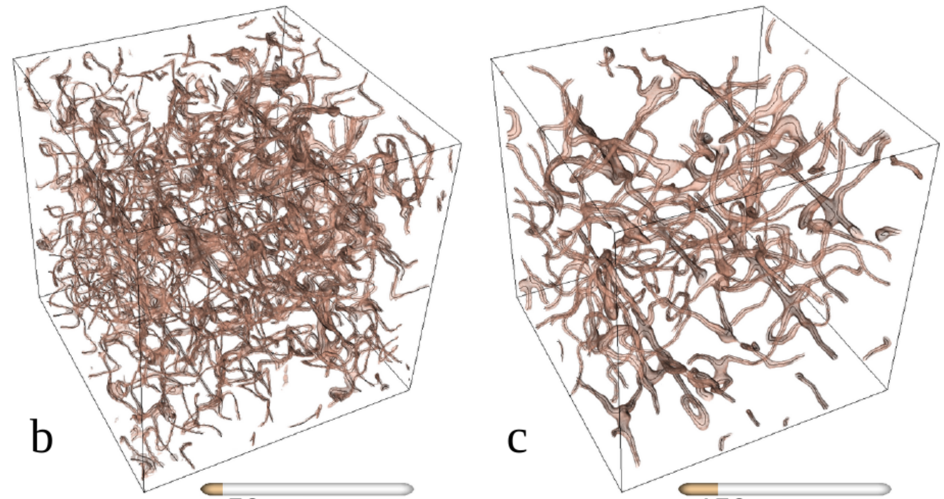

initial state:

→ zero temperature (T = 0)
→ regular lattice of imprinted vortices in all three directions
→ the lattice consists of alternately arranged vortices and anti-vortices
→ small long-wavelength perturbations of vortex lines

Calculations:

→ TDDFT for two coupling constants: $ak_F=\infty$ and $ak_F=-1.8$

→ modified GPE (Extended Thomas Fermi) for the same initial conditions

$$i\hbar e^{i\eta}\frac{\partial\psi_B(\mathbf{r},t)}{\partial t}=\left(\frac{-\hbar^2\nabla^2}{2m_B}+\mathcal{E}'\big(n_B(\mathbf{r},t)\big)\right)\psi_B(\mathbf{r},t),$$

phase factor to model dissipation

mass of dimer (2m)

effective mean-field chemical potential ($=\xi\varepsilon_F$)

PHYSICS.WUT

Quantum turbulence in 3D – observables

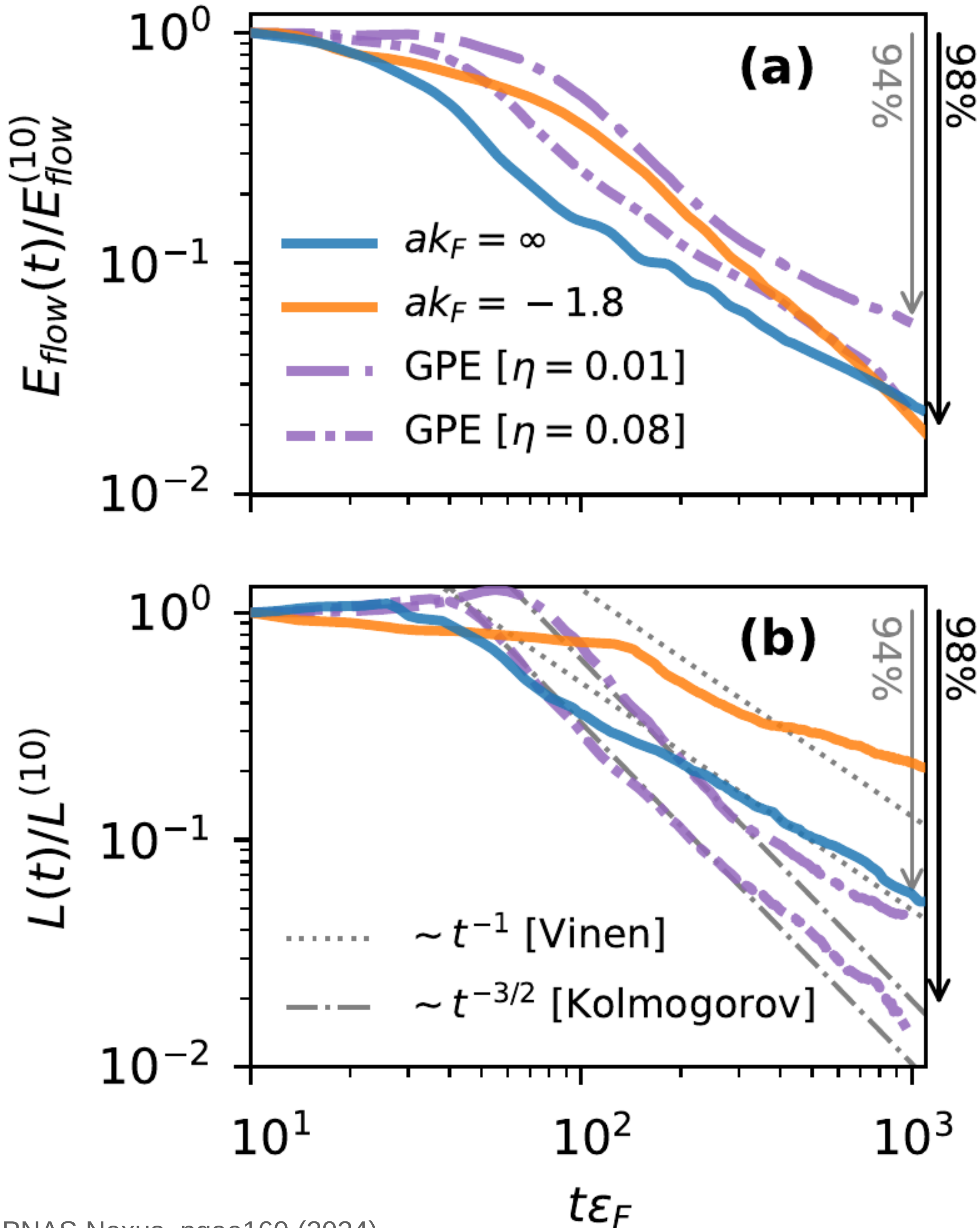

→ flow energy $E_{\text{flow}}(t) = \int \frac{\boldsymbol{j}^2(\boldsymbol{r},t)}{2n(\boldsymbol{r},t)} \mathrm{d}^3\boldsymbol{r}$,

→ total vortex length $L(t)$

$$= \int \frac{n\boldsymbol{v}^2}{2} d^3 r,$$

$$\boldsymbol{j} = n\boldsymbol{v}$$

PNAS Nexus, pgae160 (2024)

PHYSICS.WUT

Quantum turbulence in 3D – observables

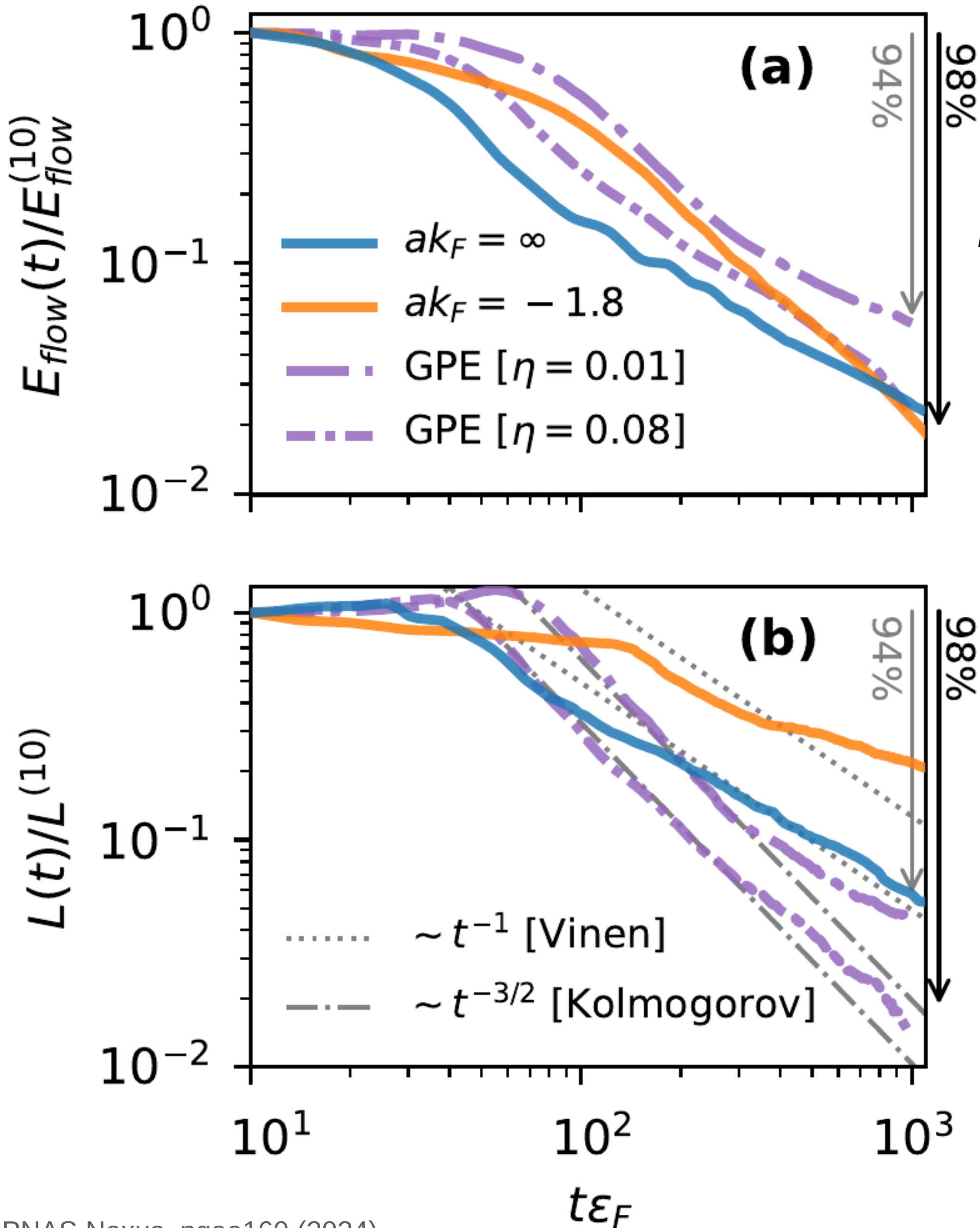

→ flow energy $E_{\text{flow}}(t) = \int \frac{\boldsymbol{j}^2(\boldsymbol{r},t)}{2n(\boldsymbol{r},t)} \mathrm{d}^3\boldsymbol{r},$

→ total vortex length $L(t)$

Helmholtz decomposition:

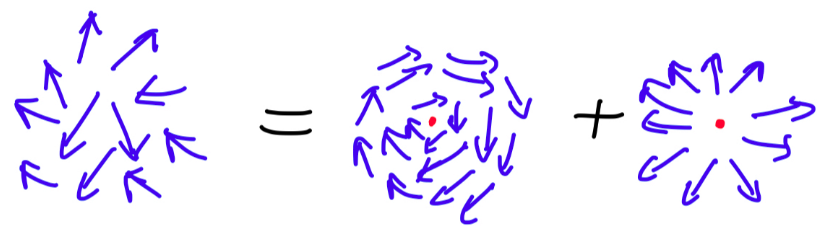

$$E_{\text{flow}} = E_{\text{flow}}^{\text{vortex}} + E_{\text{flow}}^{\text{phonon}}$$

~L(t)

$$E_{\text{flow}} \geqslant E_{\text{flow}}^{\text{vortex}} \Rightarrow \boxed{\frac{E_{\text{flow}}(t)}{E_{\text{flow}}(0)} \geqslant \frac{L(t)}{L(0)}}$$

PNAS Nexus, pgae160 (2024)

Quantum turbulence in 3D – observables

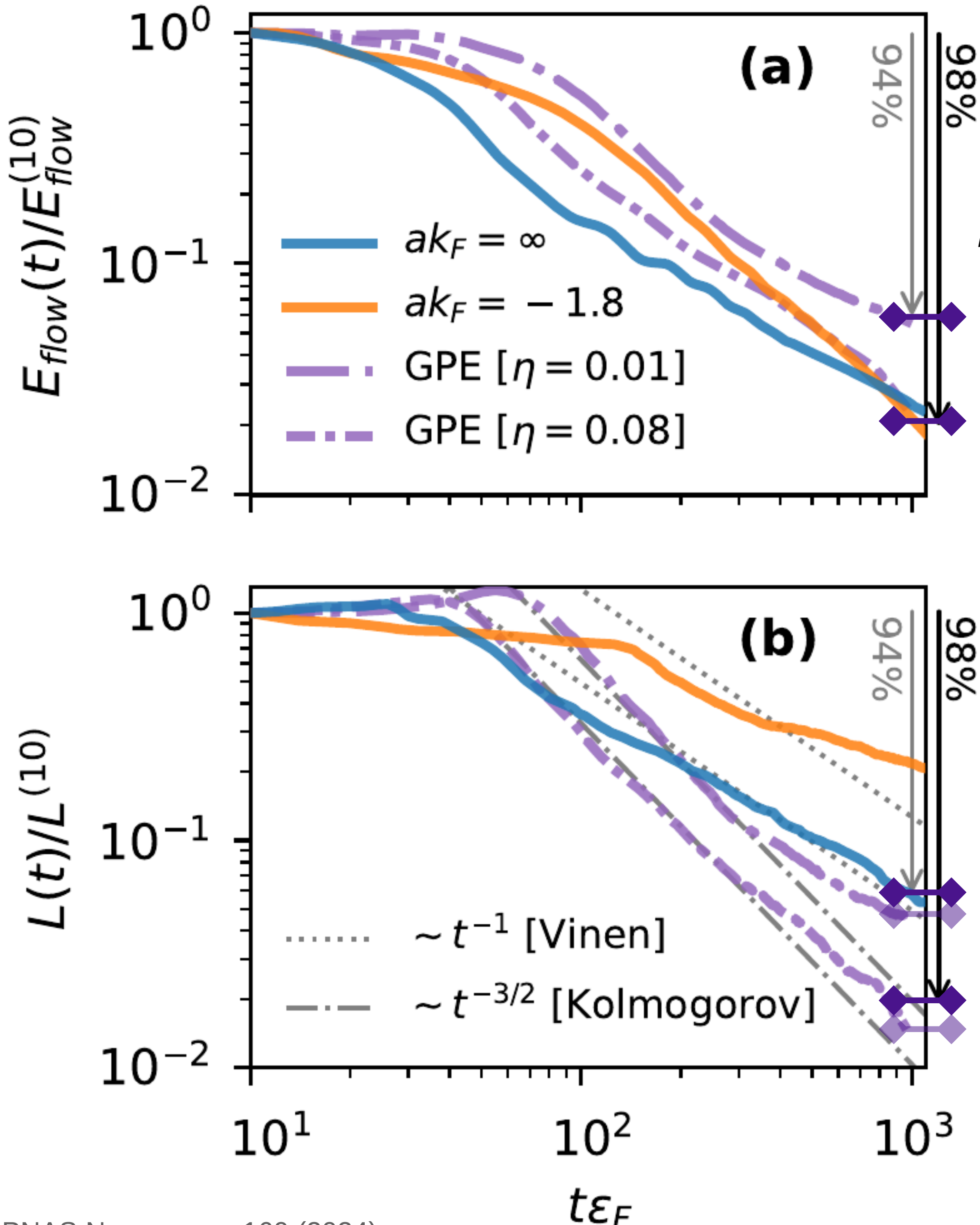

→ flow energy $E_{\text{flow}}(t) = \int \frac{\boldsymbol{j}^2(\boldsymbol{r},t)}{2n(\boldsymbol{r},t)} \mathrm{d}^3\boldsymbol{r}$,

→ total vortex length L(t)

Helmholtz decomposition:

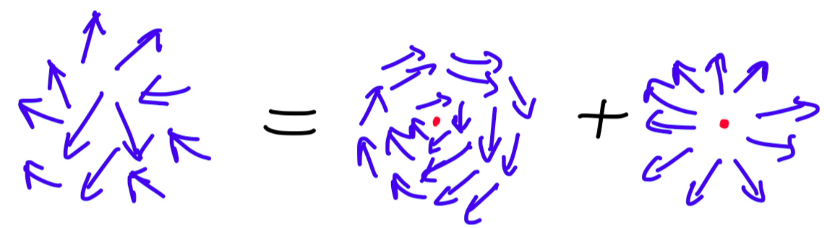

$$E_{\text{flow}} = E_{\text{flow}}^{\text{vortex}} + E_{\text{flow}}^{\text{phonon}}$$

~L(t)

$$E_{\text{flow}} \geqslant E_{\text{flow}}^{\text{vortex}} \Rightarrow \boxed{\frac{E_{\text{flow}}(t)}{E_{\text{flow}}(0)} \geqslant \frac{L(t)}{L(0)}}$$

→ **The expected result is observed for bosonic (GPE) simulations...**

PNAS Nexus, pgae160 (2024)

PHYSICS.WUT

Quantum turbulence in 3D – observables

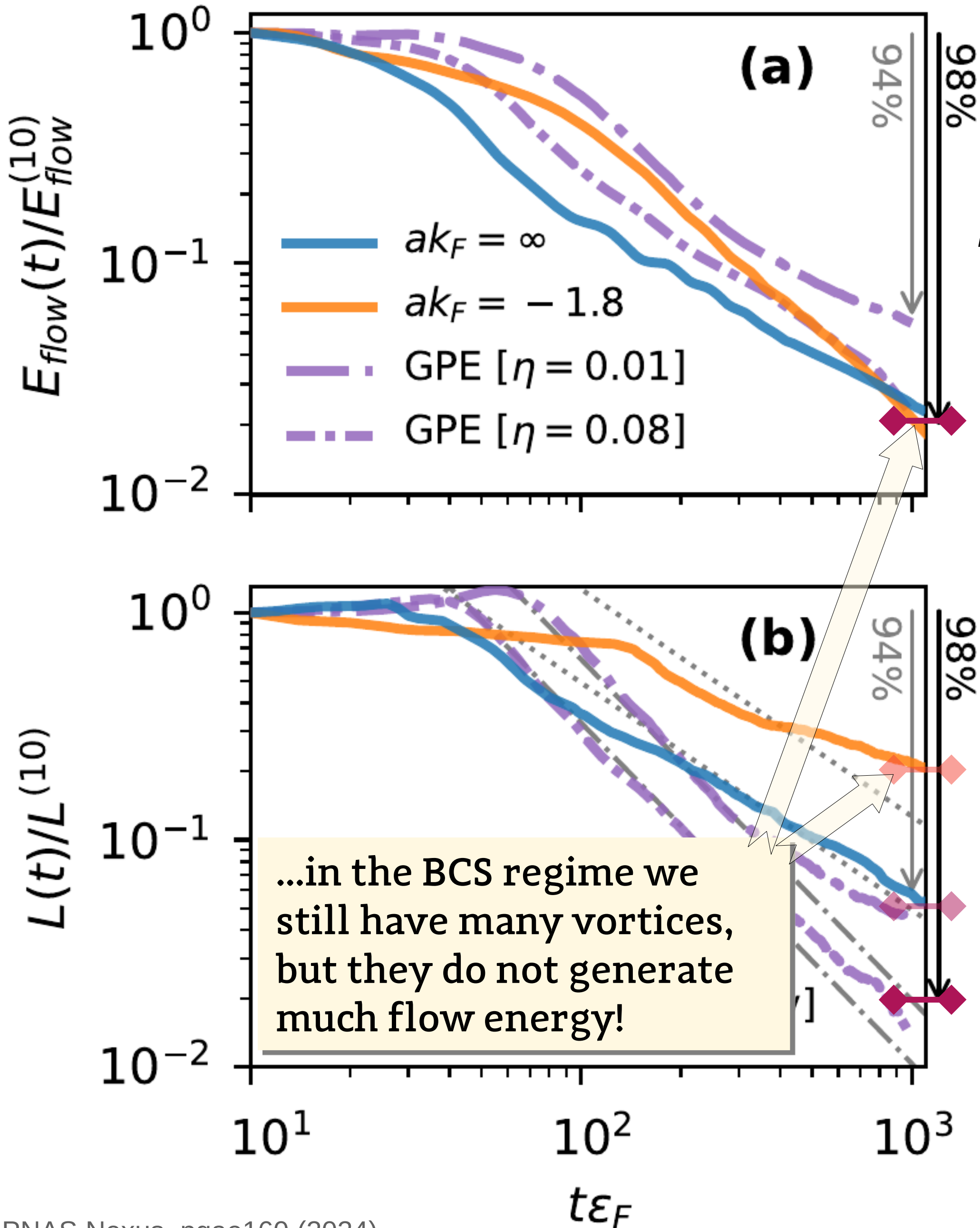

...in the BCS regime we still have many vortices, but they do not generate much flow energy!

→ flow energy $E_{\text{flow}}(t) = \int \frac{\boldsymbol{j}^2(\boldsymbol{r},t)}{2n(\boldsymbol{r},t)} \mathrm{d}^3\boldsymbol{r},$

→ total vortex length L(t)

Helmholtz decomposition:

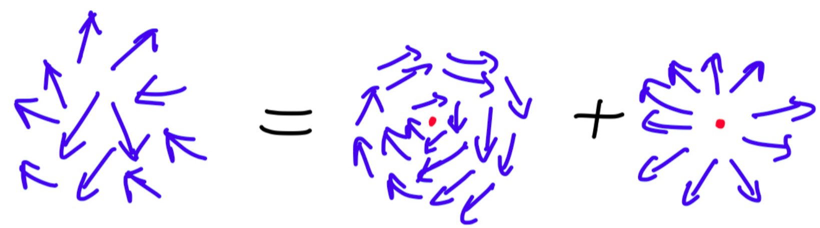

$$E_{\text{flow}} = E_{\text{flow}}^{\text{vortex}} + E_{\text{flow}}^{\text{phonon}}$$

~L(t)

$$E_{\text{flow}} \geqslant E_{\text{flow}}^{\text{vortex}} \Rightarrow \boxed{\frac{E_{\text{flow}}(t)}{E_{\text{flow}}(0)} \geqslant \frac{L(t)}{L(0)}}$$

→ **The expected result is observed for bosonic (GPE) simulations...**

→ **but for fermionic simulations (TDDFT) there is qualitatively different behavoir!**

PNAS Nexus, pgae160 (2024)

PHYSICS.WUT

Quantum turbulence in 3D – observables

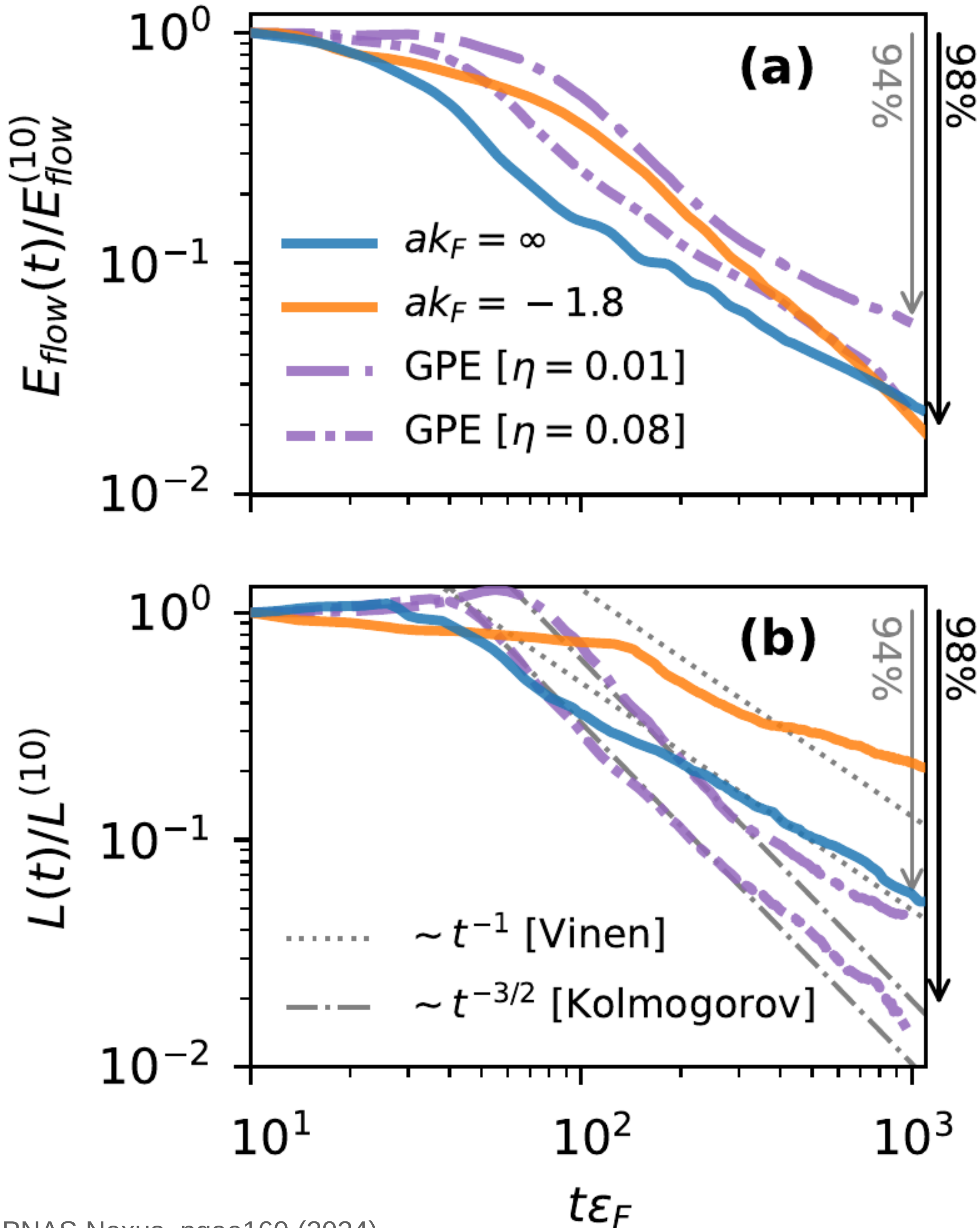

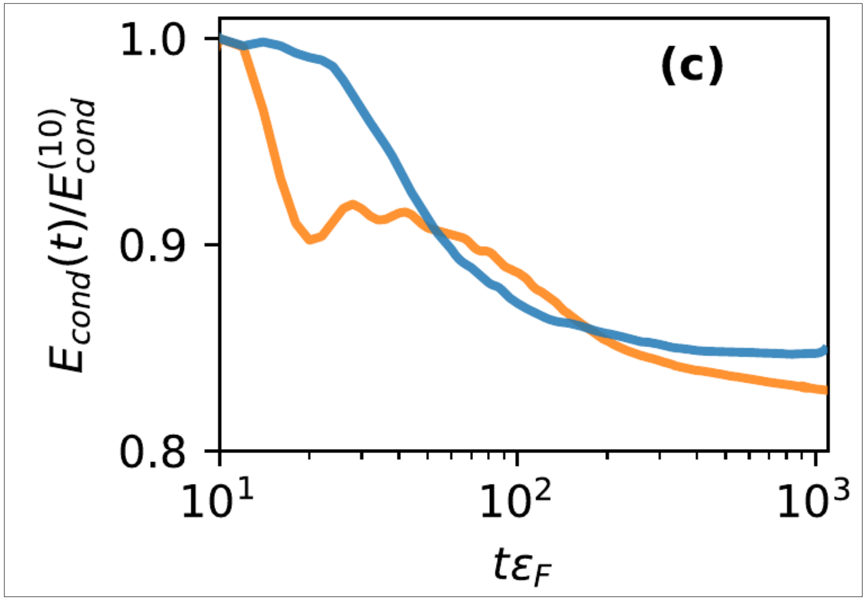

$$E_{\mathrm{BCS}} = E_{\mathrm{FG}} - \frac{3|\Delta|^2}{8\varepsilon_F}N$$

$$E_{\mathrm{cond}} = \int \frac{3}{8}\frac{|\Delta(\mathbf{r})|^2}{\varepsilon_F(\mathbf{r})} n(\mathbf{r})d\mathbf{r}$$

… we observed that the Cooper pairs condensate is depleted during the evolution... → **pair breaking!**

PNAS Nexus, pgae160 (2024)

PHYSICS.WUT

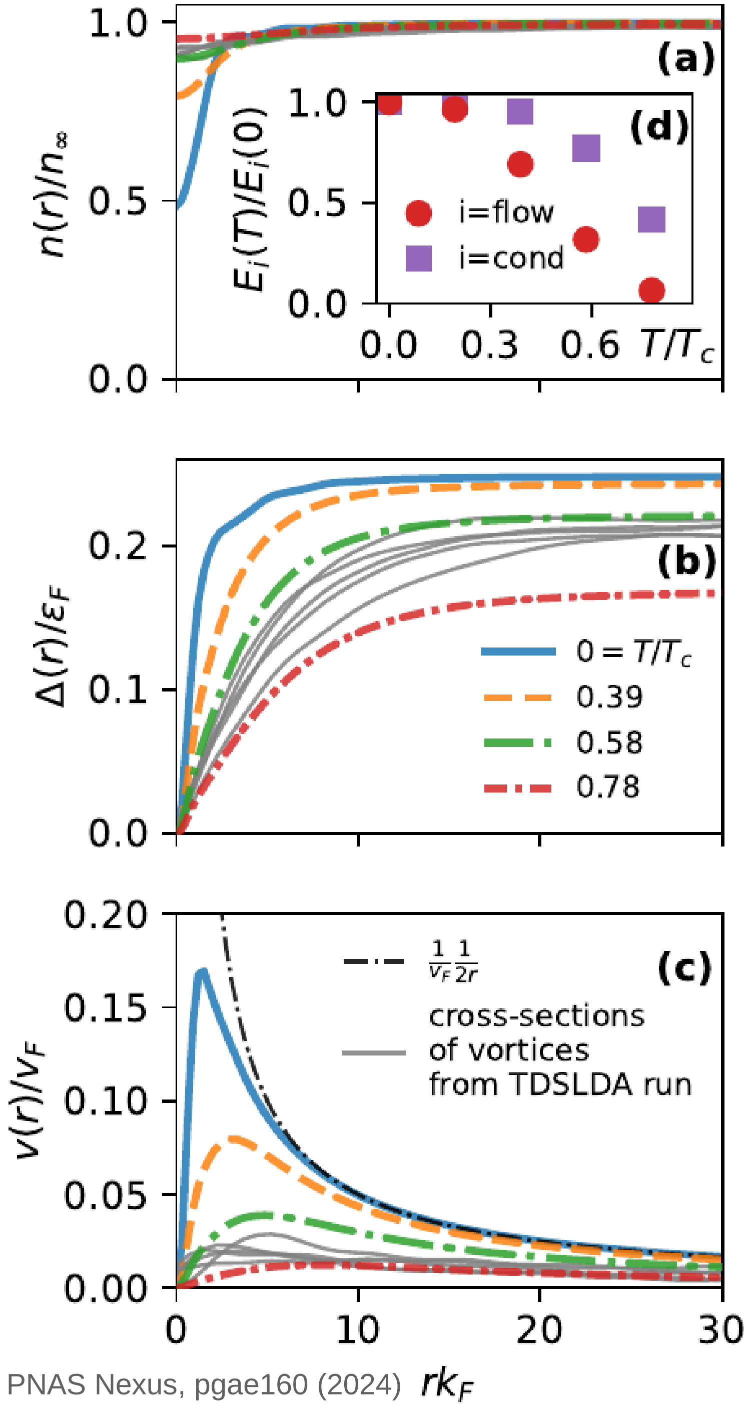

Radial dependence of the:

(a) density n(r),

(b) order parameter Δ(r),

(c) velocity v(r) = j(r)/n(r)

for a single straight vortex line

at various temperatures in the BCS regime ($k_Fa = -1.8$).

PNAS Nexus, pgae160 (2024)

PHYSICS.WUT

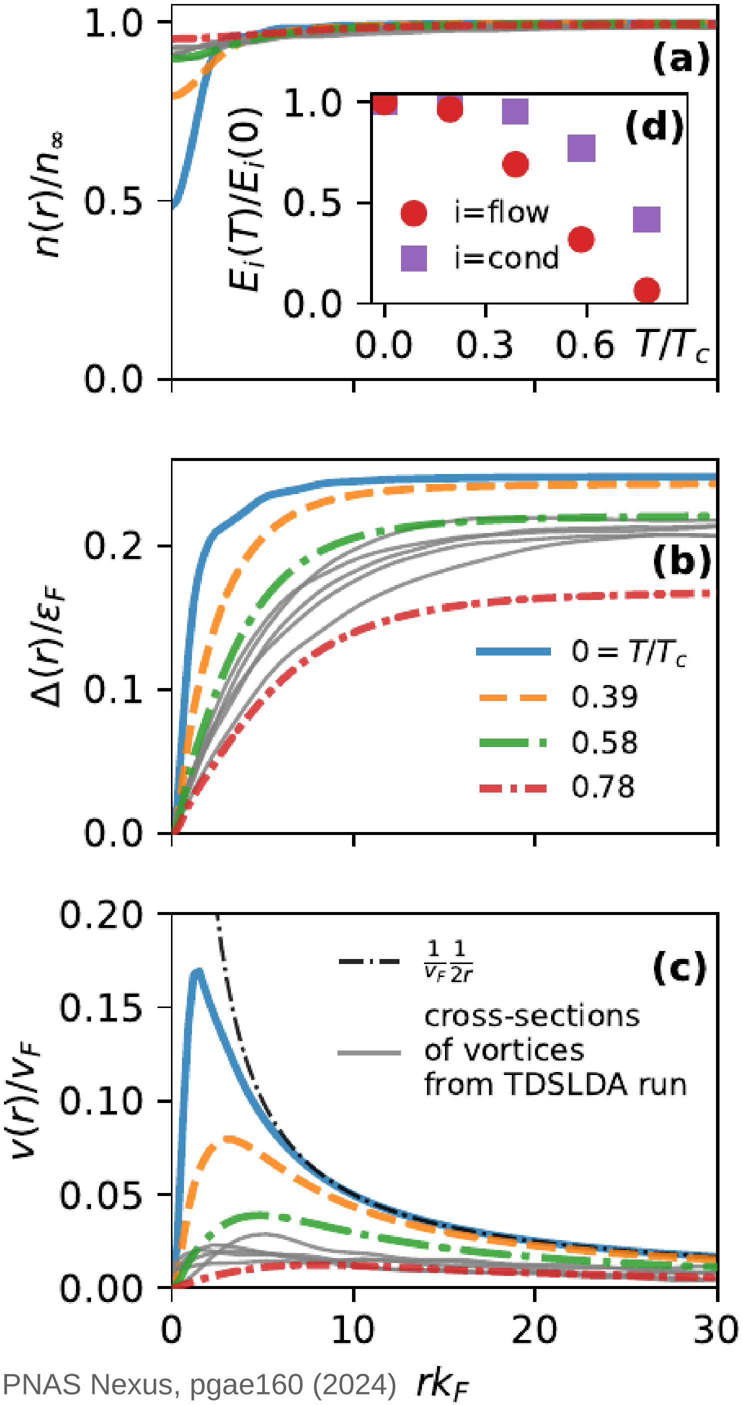

Radial dependence of the:

(a) density n(r),

(b) order parameter Δ(r),

(c) velocity v(r) = j(r)/n(r)

for a single straight vortex line
at various temperatures in the BCS regime ($k_F a = -1.8$).

The thin gray lines show the profiles of selected vortices from the TDDFT calcs taken at time $t\varepsilon_F$ = 1,000
→ the system effectively heats up!

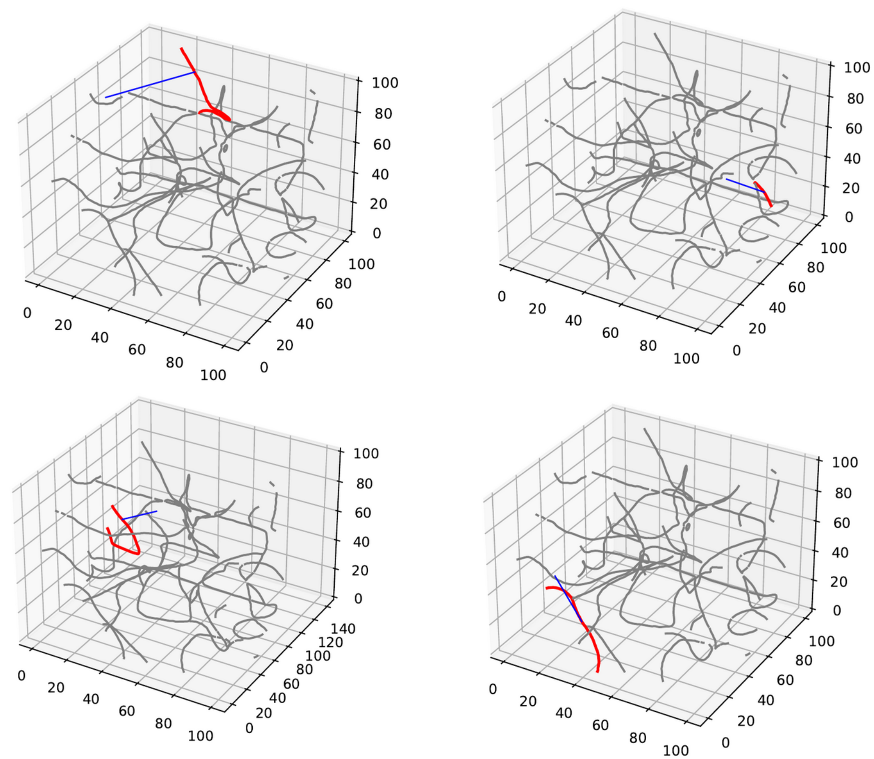

PNAS Nexus, pgae160 (2024)

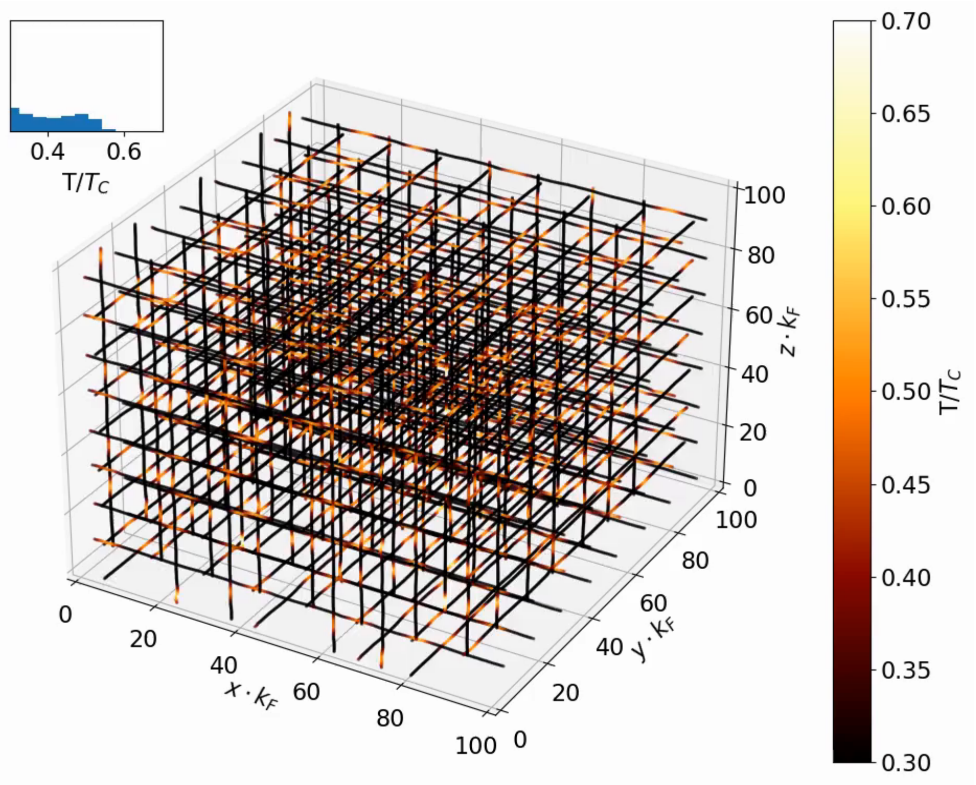

The temperature dependence of the vortex-core density n_{core} allows use fermionic vortices as a local thermometers.

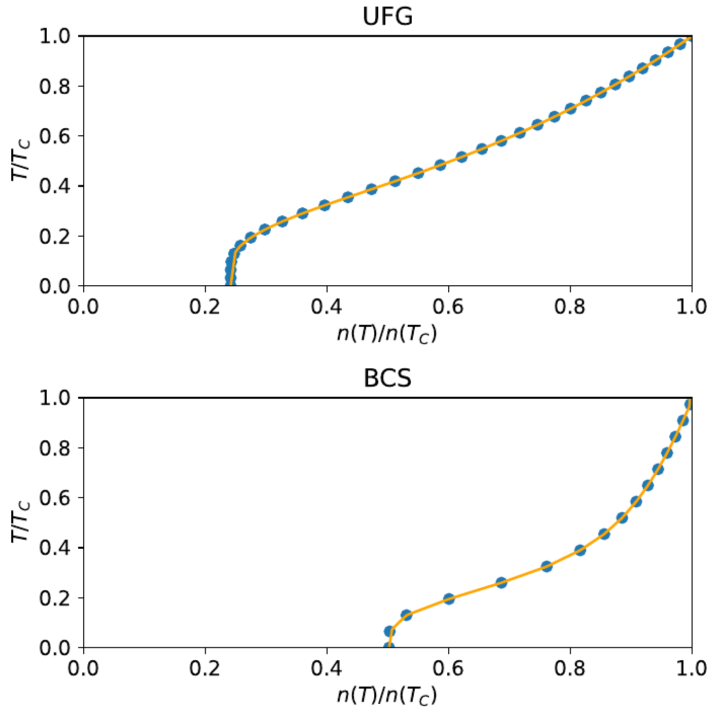

The temperature dependence of the vortex-core density n_{core} allows use fermionic vortices as a local thermometers.

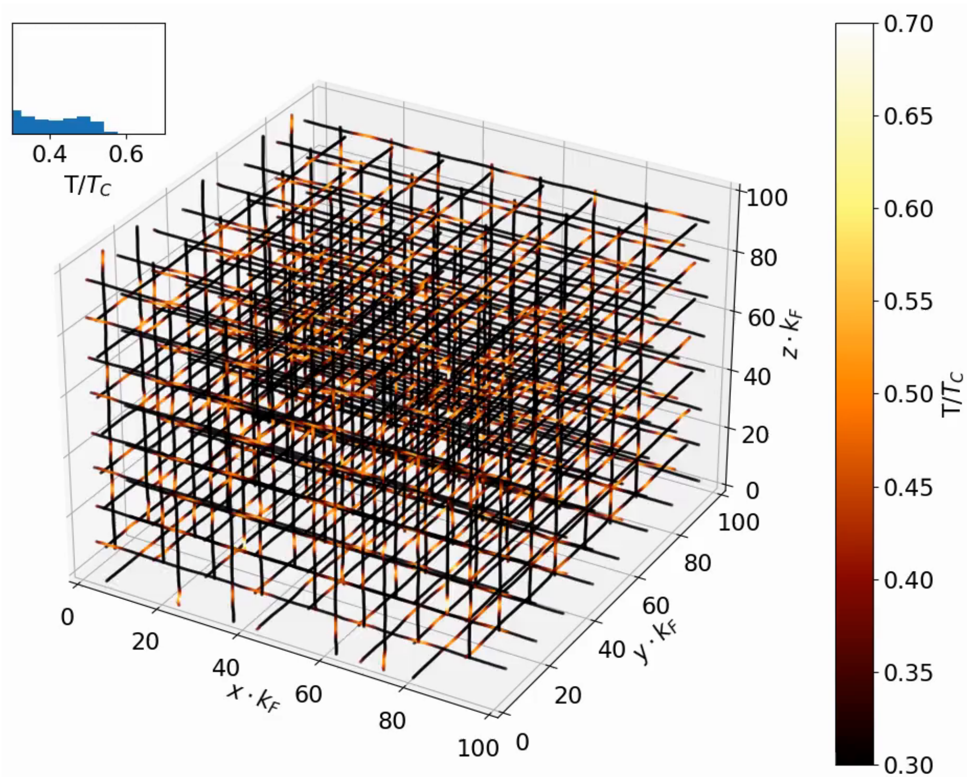

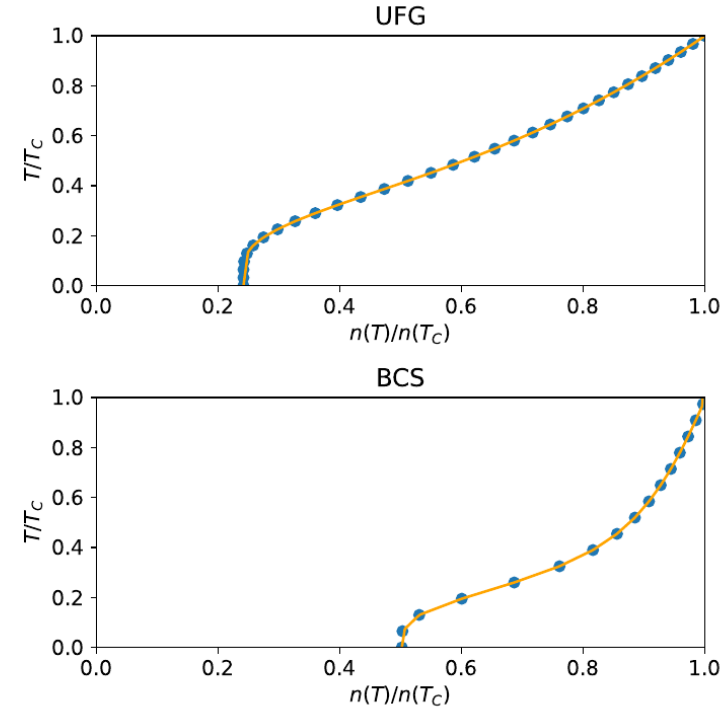

→ the effective temperature of vortex lines is higher in regions of higher curvature (reconnections, kelvin waves)

→ similarity to the heating of wire, which is sharply bent back and forth...

→ … also to mechanism proposed by Silaev.

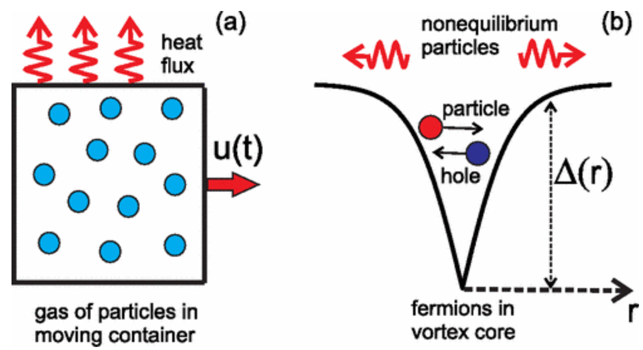

Fig. from: M.A. Silaev, *Universal Mechanism of Dissipation in Fermi Superfluids at Ultralow Temperatures,* Phys. Rev. Lett. 108, 045303 (2012)

PNAS Nexus, pgae160 (2024)

GPE: $\boldsymbol{j} = n\boldsymbol{v}_s = n\frac{\hbar}{M}\nabla\phi, \quad n = |\psi|^2,\ \phi = \arg(\psi)$

DFT: $\boldsymbol{j} \neq n\boldsymbol{v}_s = n\frac{\hbar}{M}\nabla\phi, \quad n = \sum_{E_n>0} |v_n|^2,\ \phi = \arg(\Delta),\ M = 2m$

In this plot: v(r) = j(r)/n(r)

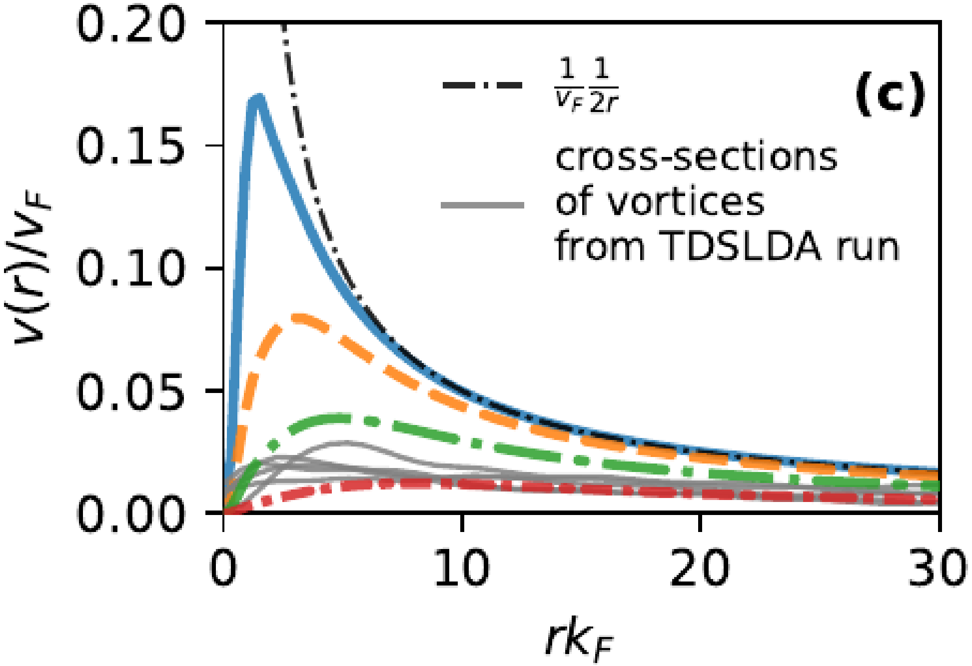

PHYSICS.WUT

GPE: $\boldsymbol{j} = n\boldsymbol{v}_s = n\dfrac{\hbar}{M}\nabla\phi, \quad n = |\psi|^2,\ \phi = \arg(\psi)$

DFT: $\boldsymbol{j} \neq n\boldsymbol{v}_s = n\dfrac{\hbar}{M}\nabla\phi, \quad n = \sum_{E_n>0} |v_n|^2,\ \phi = \arg(\Delta),\ M = 2m$

In general: $\boldsymbol{j} = \underbrace{n_s\boldsymbol{v}_s}_{superfluid} + \underbrace{n_n\boldsymbol{v}_n}_{normal}$

One should define n_s or n_n not directly via the quantum wave-function, but as the response to the external perturbation, like a "phase twist".

PHYSICS.WUT

GPE: $\boldsymbol{j} = n\boldsymbol{v}_s = n\frac{\hbar}{M}\nabla\phi, \quad n = |\psi|^2,\ \phi = \arg(\psi)$

DFT: $\boldsymbol{j} \neq n\boldsymbol{v}_s = n\frac{\hbar}{M}\nabla\phi, \quad n = \sum_{E_n>0} |v_n|^2,\ \phi = \arg(\Delta),\ M = 2m$

In general: $\boldsymbol{j} = n_s\boldsymbol{v}_s + n_n\boldsymbol{v}_n$

superfluid *normal*

One should define n_s or n_n not directly via the quantum wave-function, but as the response to the external perturbation, like a "phase twist".

Example:

1. Start with the static solution with **j**=0,
2. Imprint the phase pattern $\phi(\mathbf{r}) \rightarrow v_s = \hbar/M\, \nabla\phi$
3. Measure the current j (phase imprint should induce only superfow) $\rightarrow n_s = j/v_s$
4. Extract the normal density as $n_n = n - n_s$

See also G. Orso & S. Stringari, Phys. Rev. A 109, 023301 (2024) for formal definition of the superfluid fraction

Numerical result from DFT [ak_F=-0.70, T=0]

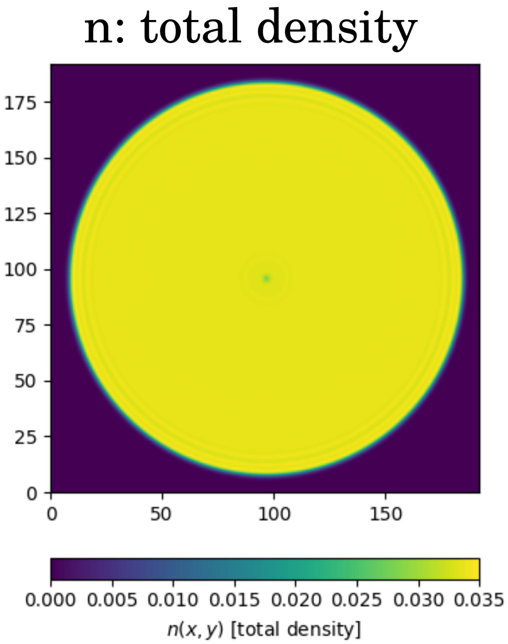

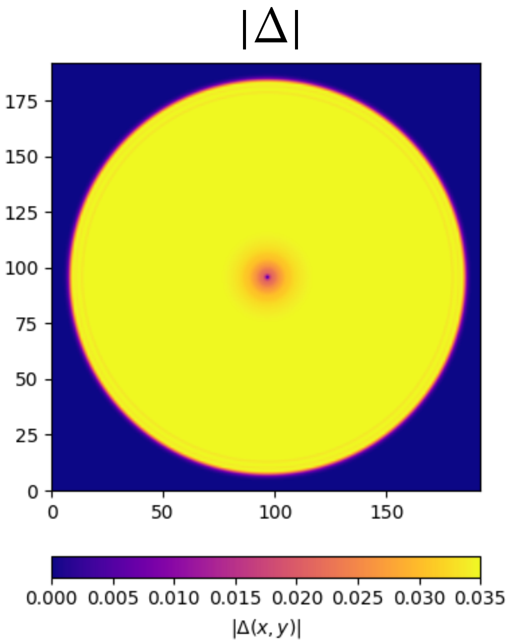

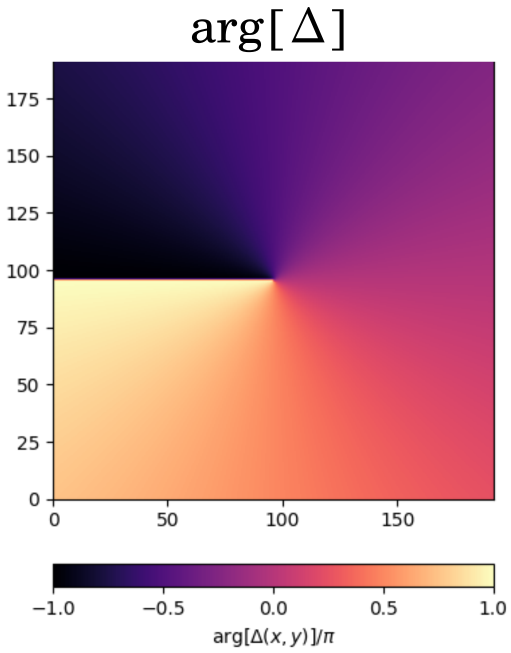

Numerical result from DFT [ak_F=-0.70, T=0]

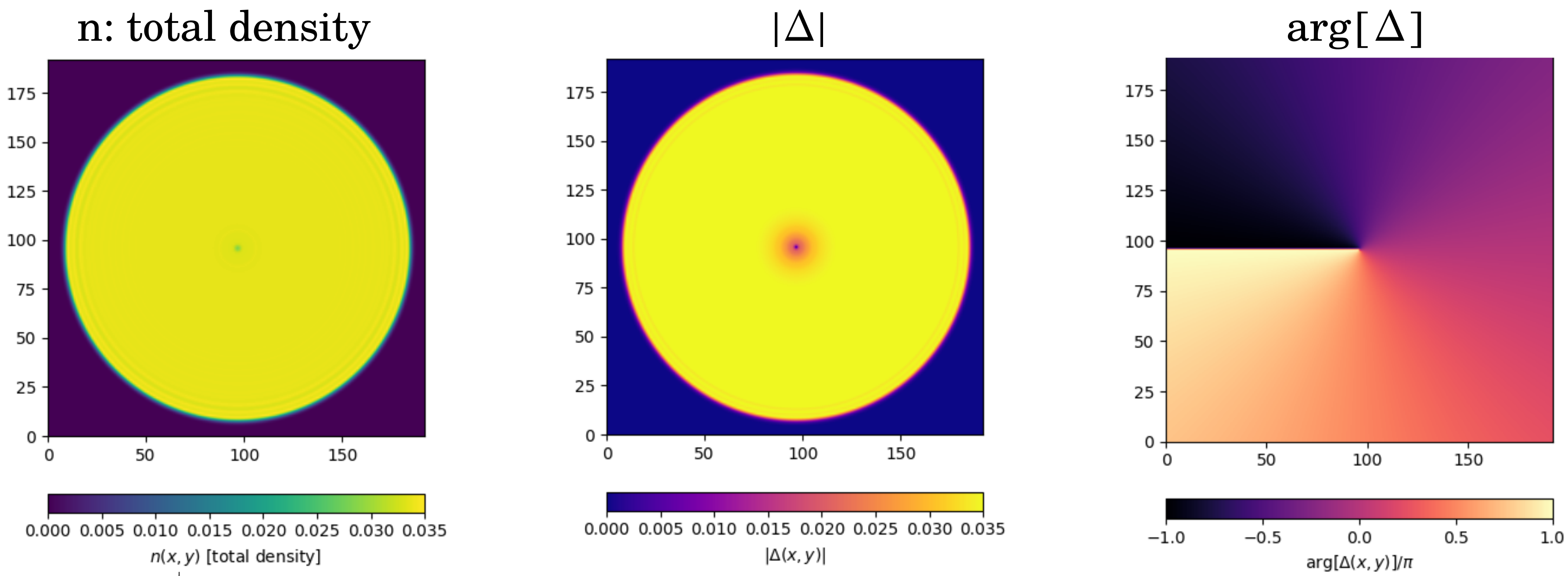

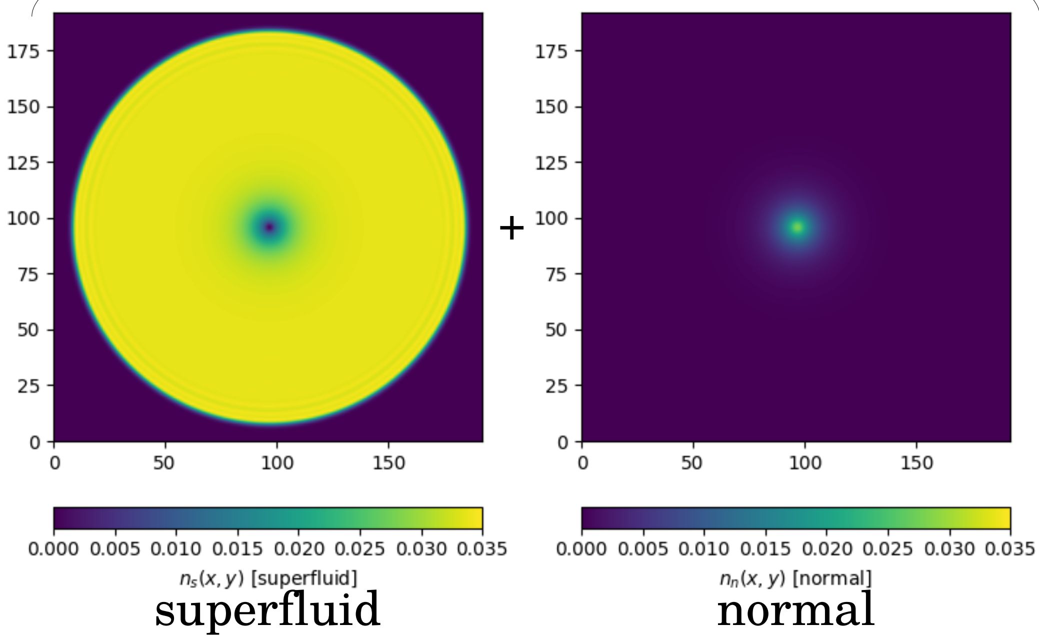

The vortex cores in Fermi superfluids are filled with the normal component, even at zero temperature!

Numerical result from finite temperature DFT [ak_F=-0.85]

Temperature enhances the normal component localized at the vortex core first...

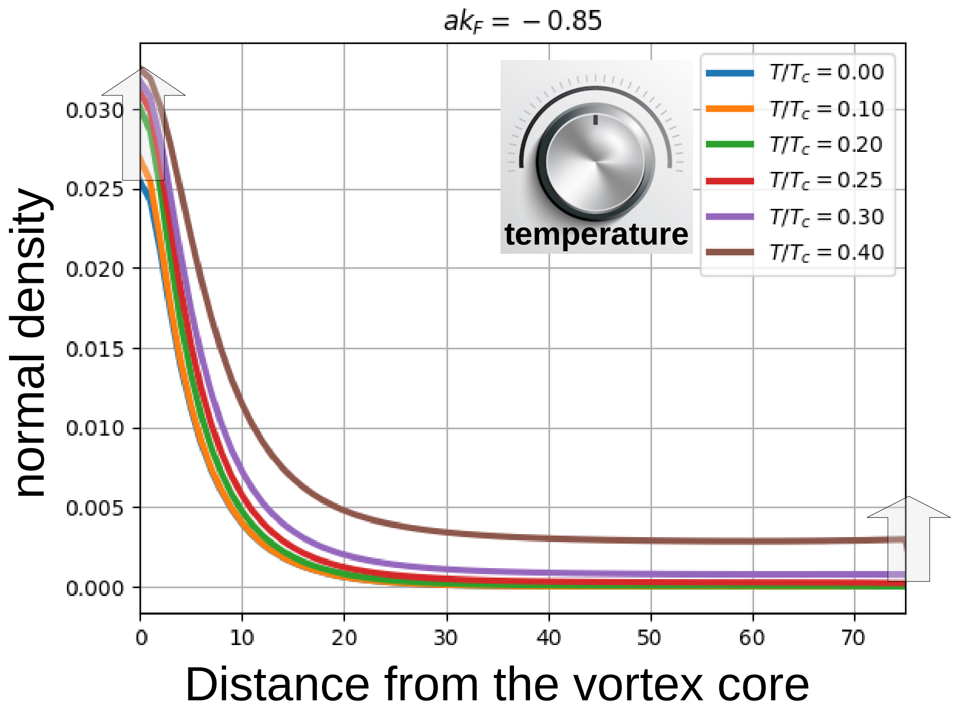

... and, for sufficiently large temperatures, also in the bulk

Numerical result from finite temperature DFT [ak_F=-0.85]

Temperature enhances the normal component localized at the vortex core first...

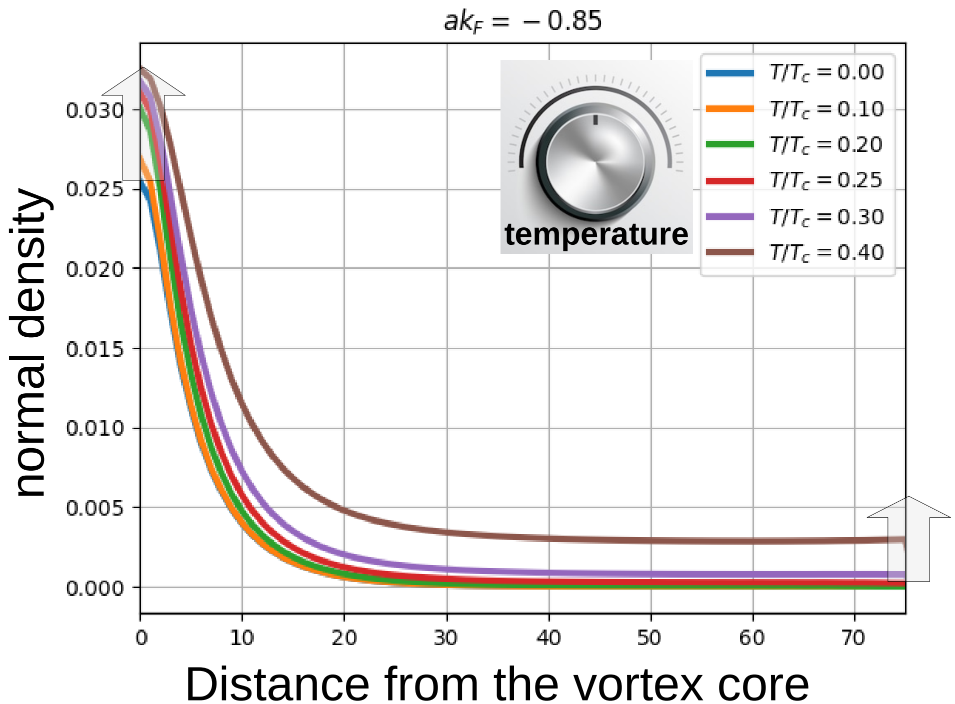

... and, for sufficiently large temperatures, also in the bulk

condensate

thermal cloud

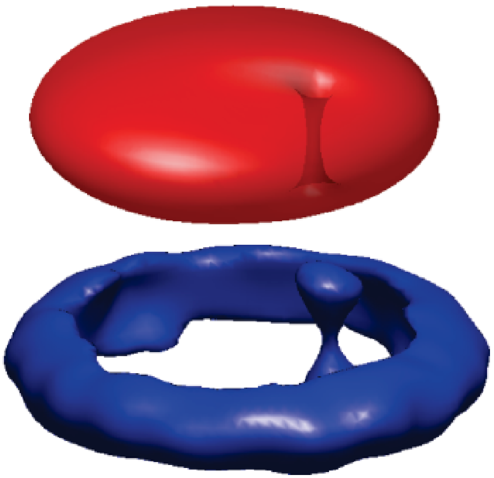

Similar effect is observed for BEC at finite T

Fig from: A. J. Allen, Phys. Rev. A 87, 013630 (2013): Zaremba, Nikuni, and Griffin (ZNG) formalism

Vortex Point Model

Source: W. J. Kwon, et.al., Nature 600, 64-69 (2021)

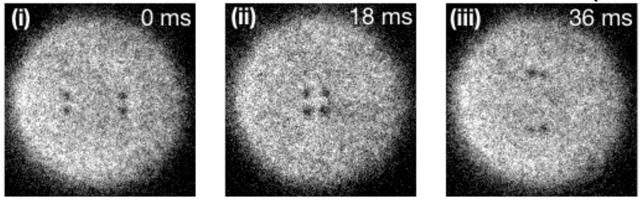

Vortex mass
in most cases the vortices are regarded as massless particles $m_V \approx 0$

$$m_V \frac{d^2 \boldsymbol{r}_V}{dt^2} = \boldsymbol{F}_{\mathrm{Magnus}} + \boldsymbol{F}_{\mathrm{boundry}} + \boldsymbol{F}_{\mathrm{dissipative}+\ldots}$$

Vortex Point Model

Source: W. J. Kwon, et.al., Nature 600, 64-69 (2021)

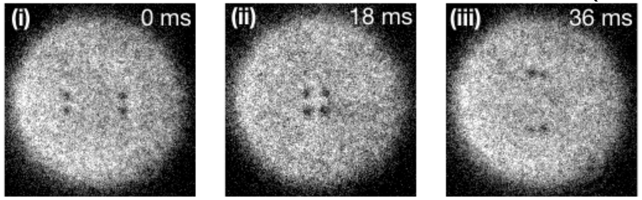

Vortex mass

in most cases the vortices are regarded as massless particles $m_V \approx 0$

$$m_V \frac{d^2 \boldsymbol{r}_V}{dt^2} = \boldsymbol{F}_{\mathrm{Magnus}} + \boldsymbol{F}_{\mathrm{boundry}} + \boldsymbol{F}_{\mathrm{dissipative+...}}$$

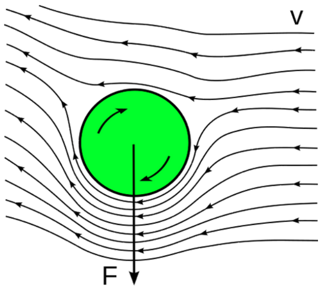

$$\mathbf{F}_{\mathrm{Magnus}} = n_s \kappa\, \hat{\mathbf{z}} \times (\mathbf{v}_V - \mathbf{v}_s)$$

Biot–Savart Law in 2D

Superflow is generated by all other vortices

$$\mathbf{v}_s(\mathbf{r}) = \frac{\kappa}{2\pi} \sum_{j \neq i} \frac{\hat{\mathbf{z}} \times (\mathbf{r} - \mathbf{r}_j)}{|\mathbf{r} - \mathbf{r}_j|^2}$$

Vortex Point Model

Source: W. J. Kwon, et.al., Nature 600, 64-69 (2021)

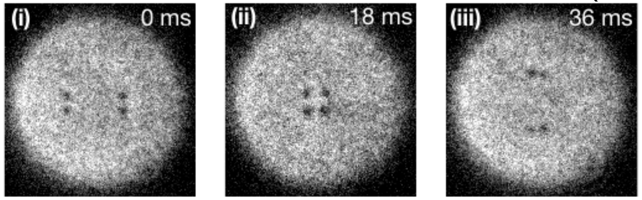

Vortex mass
in most cases the vortices are regarded as massless particles $m_V \approx 0$

$$m_V \frac{d^2 \boldsymbol{r}_V}{dt^2} = \boldsymbol{F}_{\mathrm{Magnus}} + \boldsymbol{F}_{\mathrm{boundry}} + \boldsymbol{F}_{\mathrm{dissipative+...}}$$

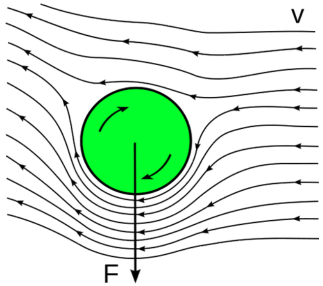

$$\mathbf{F}_{\mathrm{Magnus}} = n_s \kappa\, \hat{\mathbf{z}} \times (\mathbf{v}_V - \mathbf{v}_s)$$

Flow must be tangential to the boundry: $\mathbf{v}_s \cdot \hat{n} = 0$
Can be modeled by means of image vortices.

Biot–Savart Law in 2D
Superflow is generated by all other vortices

$$\mathbf{v}_s(\mathbf{r}) = \frac{\kappa}{2\pi} \sum_{j \neq i} \frac{\hat{\mathbf{z}} \times (\mathbf{r} - \mathbf{r}_j)}{|\mathbf{r} - \mathbf{r}_j|^2}$$

Vortex Point Model

Source: W. J. Kwon, et.al., Nature 600, 64-69 (2021)

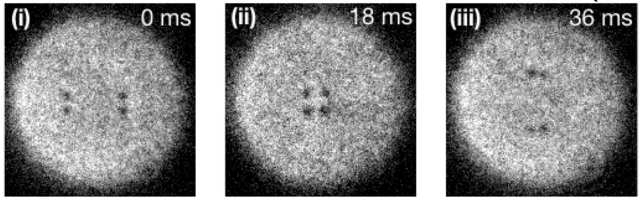

Vortex mass

in most cases the vortices are regarded as massless particles $m_V \approx 0$

$$m_V \frac{d^2 \boldsymbol{r}_V}{dt^2} = \boldsymbol{F}_{\mathrm{Magnus}} + \boldsymbol{F}_{\mathrm{boundry}} + \boldsymbol{F}_{\mathrm{dissipative}+\ldots}$$

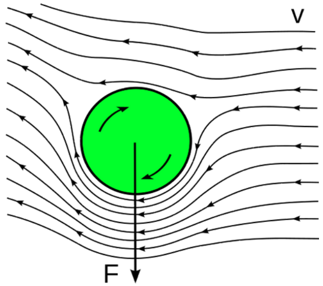

$$\mathbf{F}_{\mathrm{Magnus}} = n_s \kappa\, \hat{\mathbf{z}} \times (\mathbf{v}_V - \mathbf{v}_s)$$

Flow must be tangential to the boundry: $\mathbf{v}_s \cdot \hat{n} = 0$

Can be modeled by means of image vortices.

Interaction with n_n

In general, two components: tangential and transverse to the relative flow of the n component

$$\mathbf{F}_{\mathrm{dissipative}} = -D(\mathbf{v}_V - \mathbf{v}_n) - D' \hat{\mathbf{z}} \times (\mathbf{v}_V - \mathbf{v}_n)$$

Biot–Savart Law in 2D

Superflow is generated by all other vortices

$$\mathbf{v}_s(\mathbf{r}) = \frac{\kappa}{2\pi} \sum_{j \neq i} \frac{\hat{\mathbf{z}} \times (\mathbf{r} - \mathbf{r}_j)}{|\mathbf{r} - \mathbf{r}_j|^2}$$

Vortex mass

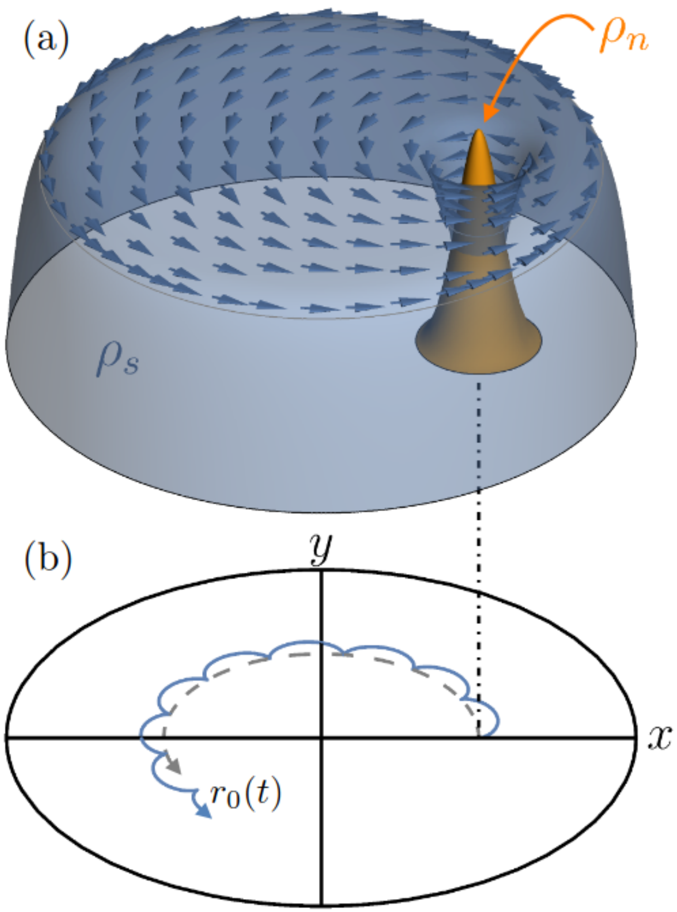

Consider: quantum vortex at disc of radius R, zero temperature limit (no dissipative forces)

$$m_V \frac{d^2 \boldsymbol{r}_V}{dt^2} = n_s \kappa\, \hat{\mathbf{z}} \times \left(\frac{d\boldsymbol{r}_V}{dt} - \mathbf{v}_s\right)$$

generated by an oppositely-charged image vortex located at position $\boldsymbol{r}_0' = (R/r_0)^2\, \boldsymbol{r}_0$ which ensures the no-flow condition across the boundary.

Related works:
T. Simula, Phys. Rev. A 97, 023609 (2018);
A. Richaud, V. Penna, and A. L. Fetter, Phys. Rev. A 103, 023311 (2021);
J. D'Ambroise et al, Phys. Rev. E 111, 034216 (2025);
A. Kanjo, H. Takeuchi, Phys. Rev. A 110, 063311 (2024);

Vortex mass

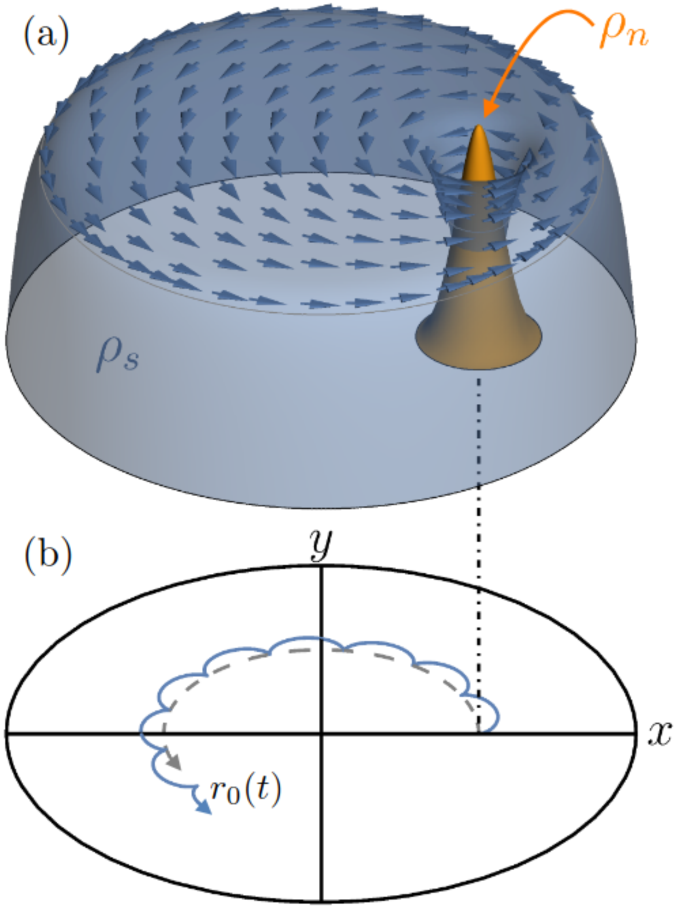

Consider: quantum vortex at disc of radius R, zero temperature limit (no dissipative forces)

$$m_V \frac{d^2 \boldsymbol{r}_V}{dt^2} = n_s \kappa \, \hat{\mathbf{z}} \times \left(\frac{d\boldsymbol{r}_V}{dt} - \mathbf{v}_s \right)$$

generated by an oppositely-charged image vortex located at position $\boldsymbol{r}_0' = (R/r_0)^2 \, \boldsymbol{r}_0$ which ensures the no-flow condition across the boundary.

If m_V=0: first order PDE $r(t) = r_0$ **(circular orbit)**

Related works:
T. Simula, Phys. Rev. A 97, 023609 (2018);
A. Richaud, V. Penna, and A. L. Fetter, Phys. Rev. A 103, 023311 (2021);
J. D'Ambroise et al, Phys. Rev. E 111, 034216 (2025);
A. Kanjo, H. Takeuchi, Phys. Rev. A 110, 063311 (2024);

Vortex mass

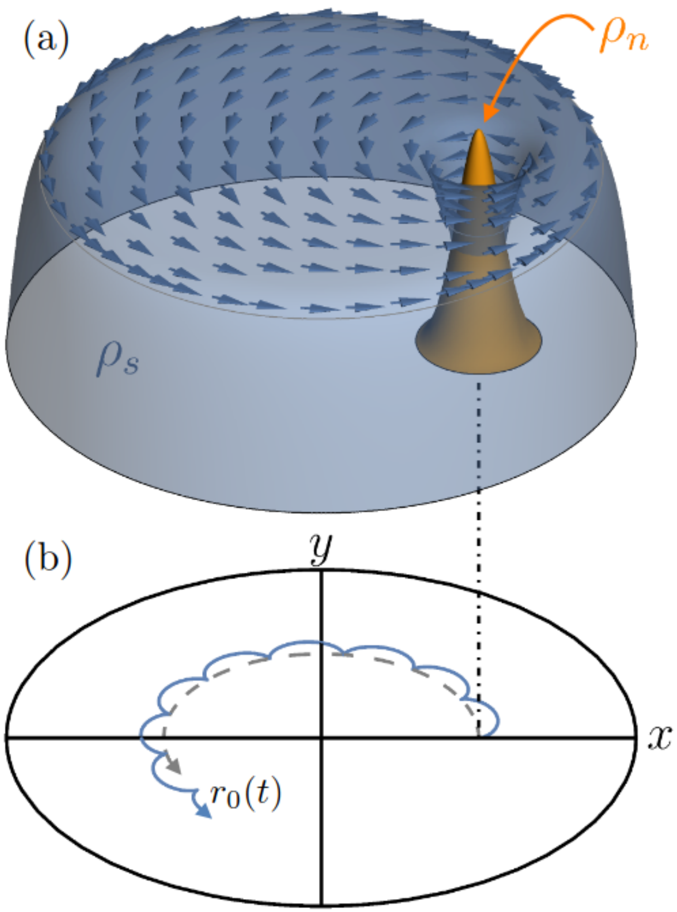

Consider: quantum vortex at disc of radius R, zero temperature limit (no dissipative forces)

$$m_V \frac{d^2 \boldsymbol{r}_V}{dt^2} = n_s \kappa \, \hat{\mathbf{z}} \times \left(\frac{d\boldsymbol{r}_V}{dt} - \mathbf{v}_s \right)$$

generated by an oppositely-charged image vortex located at position $\boldsymbol{r}_0' = (R/r_0)^2 \, \boldsymbol{r}_0$ which ensures the no-flow condition across the boundary.

If m_V=0: first order PDE $r(t) = r_0$ **(circular orbit)**

If m_V>0: second order PDE:

$$r(t) = r_0 + A(v_0, \mathfrak{m}) \sin(\omega(\mathfrak{m})t)$$

$$\mathfrak{m} = \frac{m_V}{M_s}, \quad M_s = \int n_s(\boldsymbol{r}) \, \mathrm{d}\boldsymbol{r}$$

(+ transverse oscillations)

Related works:
T. Simula, Phys. Rev. A 97, 023609 (2018);
A. Richaud, V. Penna, and A. L. Fetter, Phys. Rev. A 103, 023311 (2021);
J. D'Ambroise et al, Phys. Rev. E 111, 034216 (2025);
A. Kanjo, H. Takeuchi, Phys. Rev. A 110, 063311 (2024);

Vortex mass: numerical simulation with time-dependent DFT

A. Richaud M. Caldara, M. Capone, P. Massignan, G. Wlazłowski, arXiv:2410.12417

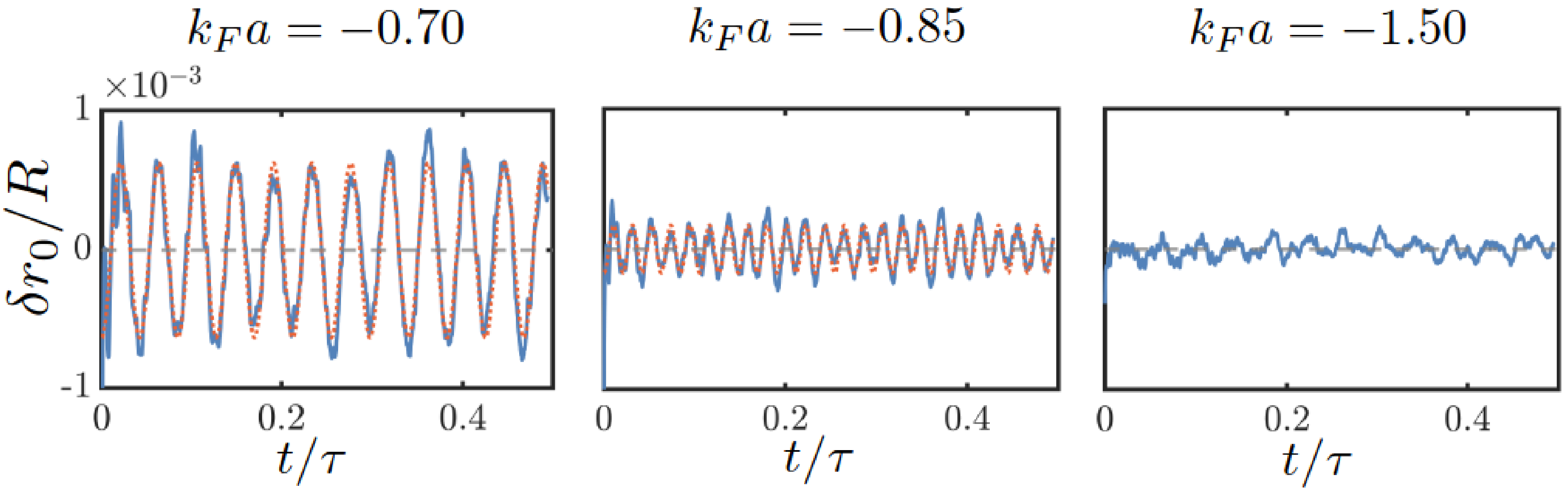

Blue: numerical result for distance of vortex core from the disk center; Orange: fit of sin function

Vortex mass: numerical simulation with time-dependent DFT

A. Richaud M. Caldara, M. Capone, P. Massignan, G. Wlazłowski, arXiv:2410.12417

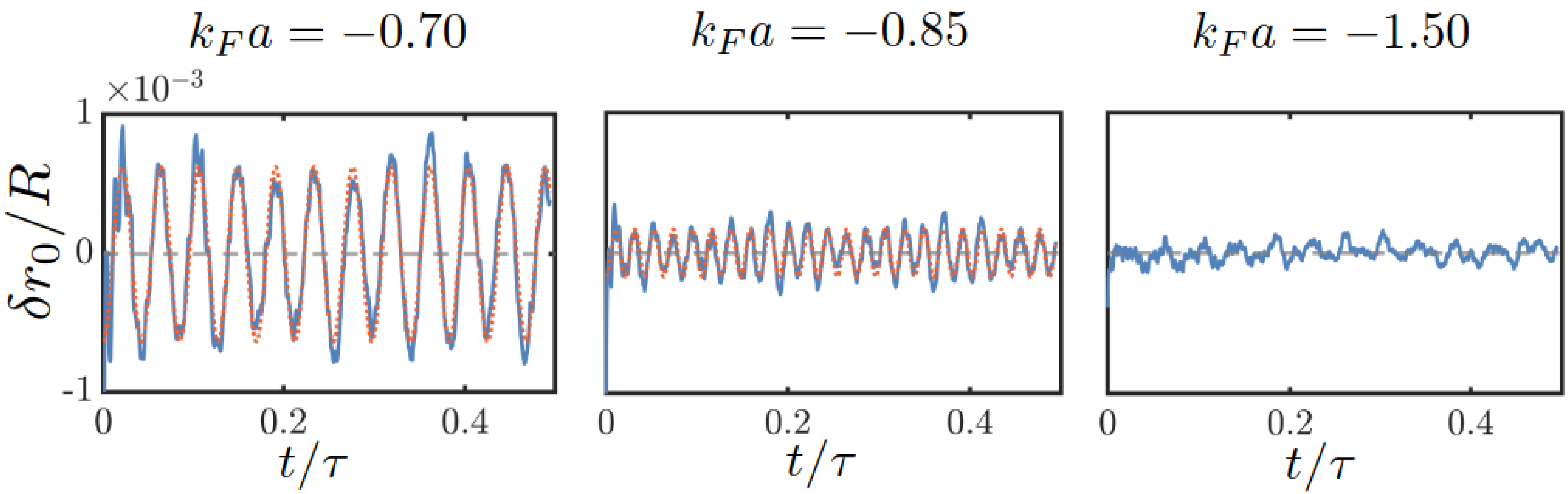

Blue: numerical result for distance of vortex core from the disk center; Orange: fit of sin function

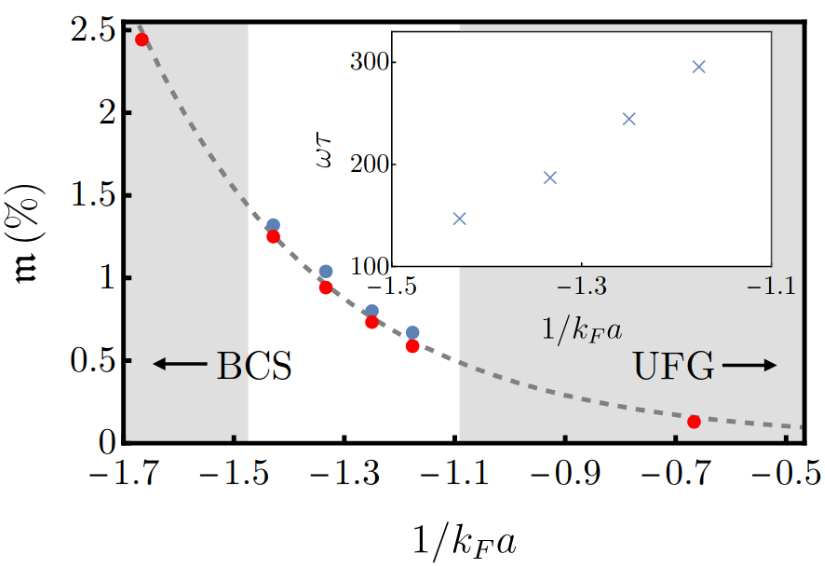

- Dynamics — Mass extracted from measurement of ω (fit of the point vortex model trajectory to data)
- N_n/N_s — Mass extracted as amount of normal component in the vortex core

Dashed line:

$$\mathfrak{m} = \alpha \times (\xi/R)^2 \qquad \xi = \frac{\hbar^2 k_F}{m\pi\bar{\Delta}},$$

vortex mass is proportional to the area of the core
(∝ ξ^2, where ξ is the coherence or healing length)

Vortex mass: numerical simulation with time-dependent DFT

A. Richaud M. Caldara, M. Capone, P. Massignan, G. Wlazłowski, arXiv:2410.12417

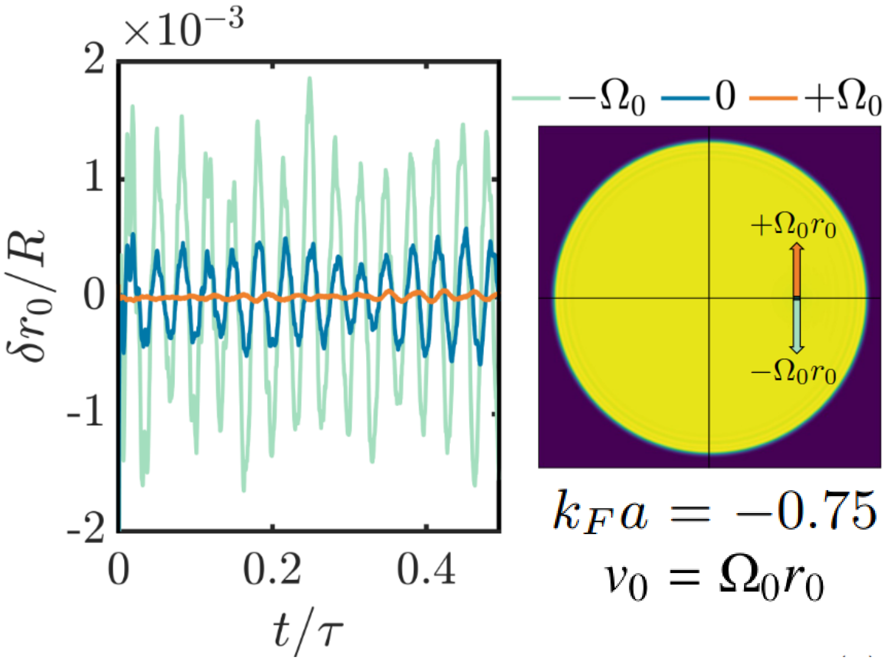

$$r(t) = r_0 + A(v_0, \mathfrak{m}) \sin(\omega(\mathfrak{m})t)$$

The sensitivity of the vortex trajectory with respect to the initial velocity is a clear indicator that the equation of motion is of the second order

Vortex mass: numerical simulation with time-dependent DFT

A. Richaud M. Caldara, M. Capone, P. Massignan, G. Wlazłowski, arXiv:2410.12417

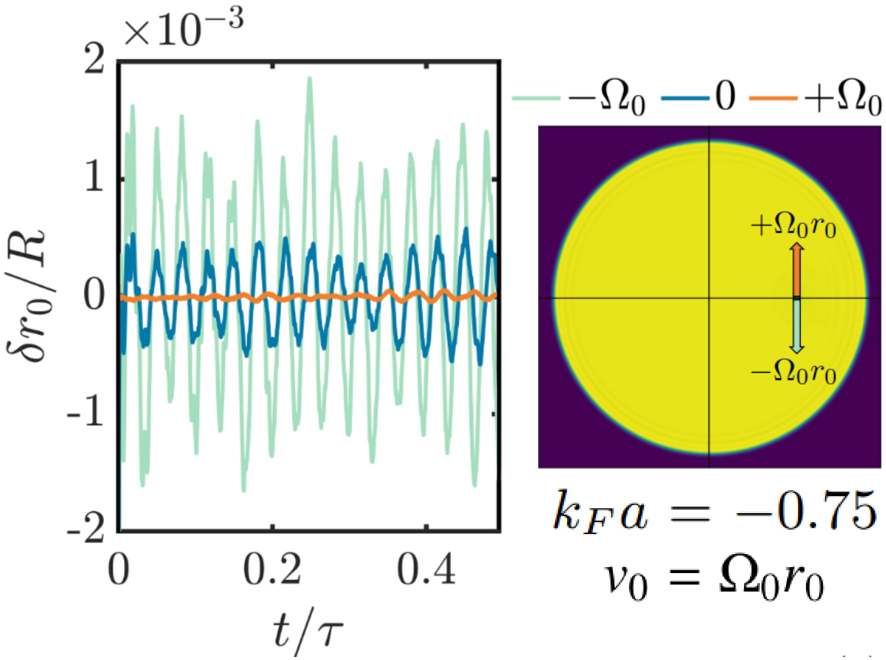

$$r(t) = r_0 + A(v_0, \mathfrak{m}) \sin(\omega(\mathfrak{m})t)$$

The sensitivity of the vortex trajectory with respect to the initial velocity is a clear indicator that the equation of motion is of the second order

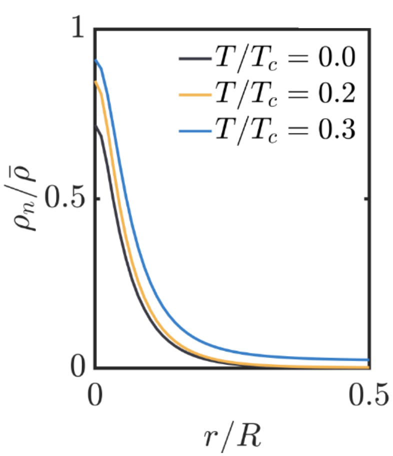

As expected,
the vortex mass grows
as we increase the
temperature.

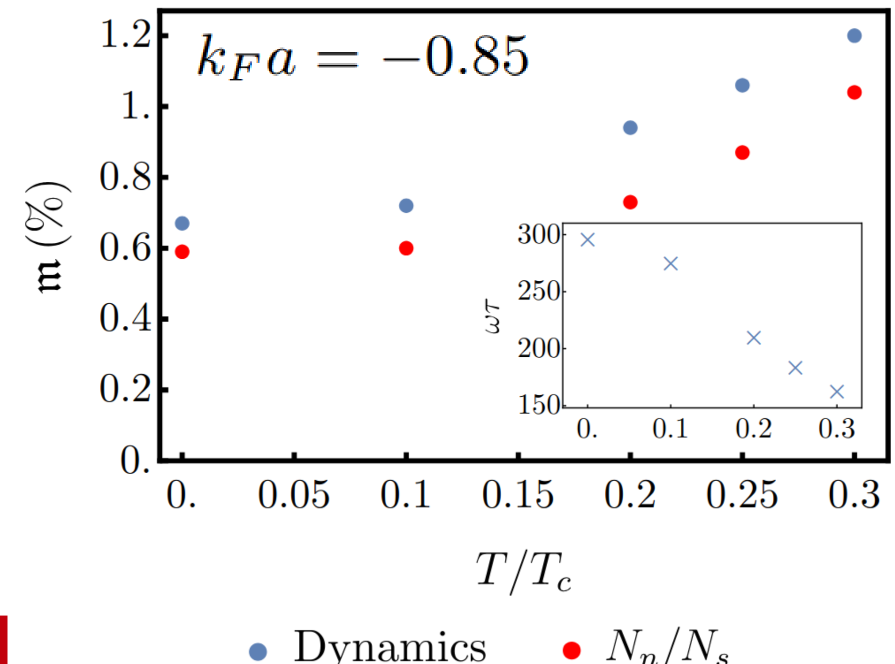

SUMMARY

- (TD)DFT is general purpose framework: it overcomes limitations of mean-field approach, while keeping numerical cost at the same level as (TD)BdG calculations.
- (TD)DFT, its implementations and HPC reached the level of maturity that allows for providing predictions for large and complex systems: ~10^4-10^5 atoms.
- Dissipation mechanisms play a key role in differentiating fermionic from bosonic turbulence:
  → *role of pair breaking mechanism (production of the "normal component") increases as we move towards BCS regime!*
- *Vortices acquire mass due to the presence of the normal component in the vortex core.*

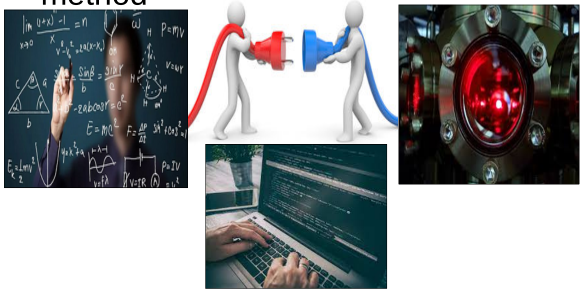

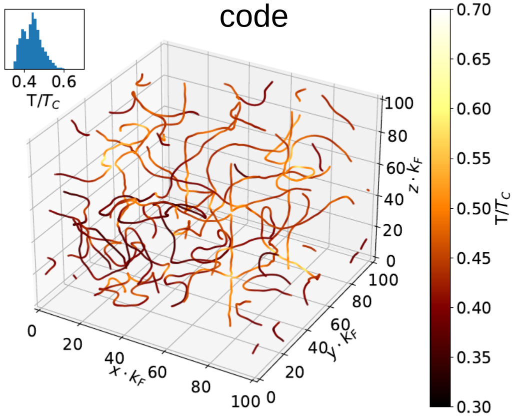

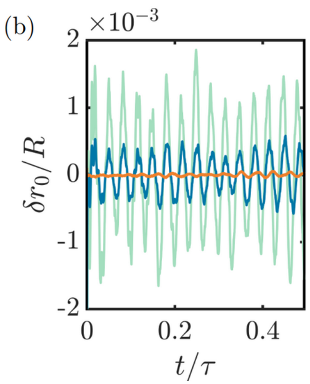

Thank you!

Collaborators:

P. Magierski, D. Pęcak, M. Tylutki, Valentin Allard, A. Makowski, A. Barresi, E. Alba, A. Zdanowicz, M. Śliwiński, D. Lazarou, (WUT);
A. Bulgac (UW);
M. Forbes, S. Sarkar (WSU);
B. Tüzemen (IFPAN)
A. Richaud, P. Massignan (UPC); M. Caldara, M. Capone (SISSA)
A. Marek (MPCDF); M. Szpindler (Cyfronet);

physics wut

Functionalities Download Gallery Publications and Materials Related projects Info EN

Warsaw University of Technology | W-SLDA Toolkit
W-BSk Toolkit

W-SLDA Toolkit

Self-consistent solver of mathematical problems which have structure formally equivalent to Bogoliubov-de Gennes equations.

static problems: st-wslda

$$\begin{pmatrix} h_a(\boldsymbol{r}) - \mu_a & \Delta(\boldsymbol{r}) \\ \Delta^*(\boldsymbol{r}) & -h_b^*(\boldsymbol{r}) + \mu_b \end{pmatrix} \begin{pmatrix} u_n(\boldsymbol{r}) \\ v_n(\boldsymbol{r}) \end{pmatrix} = E_n \begin{pmatrix} u_n(\boldsymbol{r}) \\ v_n(\boldsymbol{r}) \end{pmatrix}$$

time-dependent problems: td-wslda

$$i\hbar\frac{\partial}{\partial t}\begin{pmatrix} u_n(\boldsymbol{r},t) \\ v_n(\boldsymbol{r},t) \end{pmatrix} = \begin{pmatrix} h_a(\boldsymbol{r},t) - \mu_a & \Delta(\boldsymbol{r},t) \\ \Delta^*(\boldsymbol{r},t) & -h_b^*(\boldsymbol{r},t) + \mu_b \end{pmatrix} \begin{pmatrix} u_n(\boldsymbol{r},t) \\ v_n(\boldsymbol{r},t) \end{pmatrix}$$

Extension to nuclear matter in neutron stars

Unified solvers for static and time-dependent problems

Dimensionalities of problems: 3D, 2D and 1D

Extension to nuclear matter in neutron stars

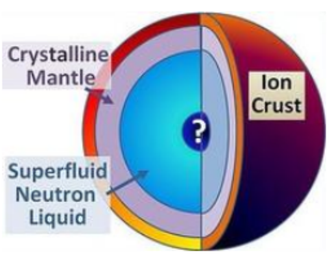

The W-SLDA Toolkit has been expanded to encompass nuclear systems, now available as the W-BSk Toolkit.

ALL FUNCTIONALITIES →

Integration with VisIt: visualization, animation and analysis tool

Speed-up calculations by exploiting High Performance Computing

Functionals for studies of BCS and unitary regimes

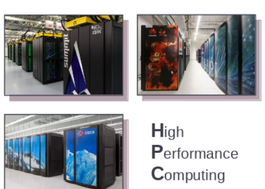

can run on "small" computing clusters as well as leadership supercomputers
(depending on the problem size)

High Performance Computing

NVIDIA CUDA AMD ROCm open source

... all tools we create for Fermi gas simulations are publicly accessible as open-source...

We release the data generated by the W-SLDA Toolkit to maximize the knowledge gained from simulations run on costly HPC systems and to share research opportunities with other groups.

September 25, 2023 (v1) | Dataset | Open

(approx 70GB of raw data)

Quantum turbulence in superfluid Fermi gas: results of numerical simulation

Gabriel Wlazłowski; Michael McNeil Forbes; Saptarshi Rajan Sarkar; and 2 others

https://zenodo.org/records/8355244

October 16, 2024 (v1) | Dataset | Open

Dynamical signature of vortex mass in Fermi superfluids: results of numerical simulations

Richaud, Andrea; Caldara, Matteo; Capone, Massimo; and 2 others

https://zenodo.org/records/13359628